THE $\mathcal{F}$-$SU(5)$ MODEL WITH VARIOUS SUPERSYMMETRY BREAKING SOFT TERMS

A Dissertation

by

DINGLI HU

Submitted to the Office of Graduate and Professional Studies of
Texas A&M University
in partial fulfillment of the requirements for the degree of

DOCTOR OF PHILOSOPHY

Chair of Committee,	Dimitri V. Nanopoulos
Committee Members,	Teruki Kamon
	Bhaskar Dutta
	Stephen A. Fulling
Head of Department,	Peter McIntyre

August 2017

Major Subject: Physics

ABSTRACT

The flipped $SU(5)$ grand unification model with additional vector-like multiplets ($\mathcal{F}$-$SU(5)$) in the framework of General No-scale Supergravity is studied. The highly constrained soft supersymmetry breaking terms of the one-parameter $\mathcal{F}$-$SU(5)$ are relaxed to allow the high-energy boundary conditions to be generically non-zero. The phenomenological viable parameter space is therefore expanded. In this project the CMSSM/mSUGRA and D-brane inspired soft supersymmetry breaking terms are implemented and studied. The non-vanishing soft terms are found to produce a broader mass range of vector-like particles and a lighter SUSY spectrum, increasing the probability that the parameter space can be probed during the LHC run 2. Both bino and higgsino dark matter are generated by this model, as well as a Higgs Funnel scenario. Particle compositions from the SUSY cascade decay modes are presented to distinguish the different scenarios phenomenologically.

DEDICATION

In memory of my grandmother, Yang Jing Yun.

Deep in my heart you will always stay.

ACKNOWLEDGMENTS

I would like to thank the chair of my advising committee, Dr. Dimitri V. Nanopoulos, for his insightful guidance in my research. He has taught me almost all my knowledge in high-energy physics.

I would also like to thank Dr. Bhaskar Dutta, Dr. Teruki Kamon, and Dr. Stephen A. Fulling for their guidance and teaching.

I also appreciate Dr. Tianjun Li and Dr. James A. Maxin for their help in fulfilling this project.

I thank the staff of Texas A&M University, especially Sherree Kessler, for their administrative help.

Special thanks to my family and friends. Their support and encouragement help me through all the difficulties in my life.

CONTRIBUTORS AND FUNDING SOURCES

Contributors

This work was supported by a dissertation committee consisting of Professors Dimitri V. Nanopoulos, Bhaskar Dutta, and Teruki Kamon of the Department of Physics and Professor Stephen A. Fulling of the Department of Mathematics.

The computing tasks for Chapter II were performed at the Tandy Supercomputing Center by Professor James A. Maxin and Mr. Adam Lux of the Department of Physics and Engineering Physics, The University of Tulsa. The analyses depicted in Chapter III were conducted in part by Professor James A. Maxin.

All other work conducted for the dissertation was completed by the student independently.

Funding Sources

Graduate study was supported by an assistantship from the Mitchell Institute.

NOMENCLATURE

SM	The Standard Model
SUSY	Supersymmetry
SUGRA	Supergravity
MSSM	Minimal Supersymmetric Standard Model
CMSSM	Constrained Minimal Supersymmetric Standard Model
mSUGRA	Minimal Supergravity
LHC	Large Hadron Collider
DM	Dark Matter

TABLE OF CONTENTS

Page

LIST OF FIGURES

FIGURE Page

LIST OF TABLES

TABLE Page

1. INTRODUCTION

We begin this chapter with a review of the Standard Model, Supersymmetry, and Supergravity. We focus on the Grand Unified Theory, especially on the $\mathcal{F}$-$SU(5)$ Model.

1.1 The Standard Model

1.1.1 Elementary Particles

The universe consists of matter. Throughout most of human history materials were thought to be continuous, and divisible however small one would like. Although there were Greek hypotheses 2,500 years ago that the division may not continue at a certain level, that is, materials have elementary constituents that cannot be separated further, or atoms for short, it was not until the 19th century that atomic hypothesis was supported by experiments. Richard P. Feynman, the 1965 Nobel laureate in physics, highly valued the importance of the atomic fact in his famous *The Feynman Lectures on Physics* [3],

> If, in some cataclysm, all of scientific knowledge were to be destroyed, and only one sentence passed on to the next generation of creatures, what statement would contain the most information in the fewest words? I believe it is the *atomic hypothesis* (or the atomic *fact*, or whatever you wish to call it) that *all things are made of atoms — little particles that move around in perpetual motion, attracting each other when they are a little distance apart, but repelling upon being squeezed into one another*. In that one sentence, you will see, there is an *enormous* amount of information about the world, if just a little imagination and thinking are applied.

Atoms are elementary at the energy scale of chemical reactions. But as the energy is elevated, subatomic particles show up. Sir Joseph John Thomson discovered the first

subatomic particle — electron, in 1897, disproving the idea that the atoms are indivisible. Lord Ernest Rutherford probed the existence of nucleus in 1909, and discovered the proton in 1917. James Chadwick discovered the neutron in 1932 under Rutherford's supervision.

The 1940s and 1950s are the golden age of subatomic physics. Many subatomic particles were discovered, including pion (pi meson, π, 1947), kaon (K meson, K, 1947), Lambda baryon (Λ, 1950), Xi baryon (Ξ, 1952), etc. The list has been continuously appended and contains hundreds of subatomic particles today.

It is necessary to classify these subatomic particles before one can study them. Some of them follow the Bose-Einstein Statistics and have integer spin; they are called bosons, including photon (γ), W and Z bosons, gluon (g), Higgs boson (h), and mesons. The rest follow the Fermi-Dirac Statistics and have half-integer[1] spin; they are called fermions. Some of fermions are not involved in the strong interaction, including electron (e), muon (μ), tau (τ), their antiparticles, and their corresponding neutrinos. They are named leptons. The rest of the fermions, *i.e.* baryons, as well as mesons are involved in the strong interaction, and are collectively called hadrons. All of the hadrons except the proton are highly unstable, that is, they can decay into other particles in a short period of time. It can be inferred that the hadrons are more likely to be composite particles, just like the nuclei. In the quark model of hadrons, their constituents, in analog with protons and neutrons in the nuclei, are quarks, including six "flavors" (Up, Down, Charm, Strange, Top, and Bottom), each having 3 "colors". Although the quarks have not been observed individually, the quark model has provided satisfactory explanations to the phenomenology of hadrons, including why the quarks are confined. Quarks are considered to be "elementary", *i.e.* they cannot be divided into smaller parts, as well as the elementary bosons and leptons mentioned above, and they are all the elementary particles as far as we know today.

The Standard Model puts these elementary particles in a decent order, as will be intro-

[1]Half-integers are numbers that can be written as $n + \frac{1}{2}$, where n is an integer.

duced next. However, we cannot answer whether there are more elementary particles, or whether some of these known elementary particles are actually divisible — the answers to these questions belong to the physics beyond the Standard Model.

In summary, the 58 distinct elementary particles in the Standard Model include 45 fermions and 13 bosons. FIG 1.1 summarizes the elementary particles. Fermions have half-integer spin, and include 36 quarks/antiquarks (6 flavors, each having 3 colors) and 9 leptons (electron, muon, and tau, their corresponding antiparticles, and their corresponding neutrinos). Bosons have integer spin, and include 12 gauge bosons and the Higgs boson. The gauge bosons include photon, W/Z bosons (W^+, W^-, and Z^0), and 8 gluons.

1.1.2 Fundamental Interactions

Each quantum state, be it an elementary particle, a composite particle, a superposition of two different particles, or any state that is well-defined in quantum mechanics, can be identified as a vector whose components are complex numbers in mathematics. These vectors have well-defined and physically-meaningful inner products. Thus, a complex complete space equipped with an inner product, or Hilbert space for short, suffices to be used as the playground of particles in quantum mechanics. A fundamental principle in quantum mechanics indicates that multiplying a state vector by a scalar factor does not change its physical reality. That is to say, a projective Hilbert space is enough to describe all physical quantum states of particles.

There are always some symmetries in the universe, that is to say, some specific transformations may be applied to the space mentioned above, while keeping the laws of physics invariant. These transformations satisfy the definition of a group, thus they form symmetry groups. Some examples are translation in time, rotation in space, rotation in isospin space, etc.

From now on we adapt the natural unit system with $\hbar = c = 1$. As a simple example,

in Quantum Electrodynamics (QED) the action that generates the Dirac equation of an electron field is

$$\mathcal{S} = \int \bar{\psi}(i\gamma^{\mu}\partial_{\mu} - m)\psi \mathrm{d}^4 x \tag{1.1}$$

which is invariant under the transformation

$$\psi \mapsto e^{i\theta}\psi \tag{1.2}$$

that is to say, the action remains invariant with a change in the phase angle θ. Since the change of θ is a rotation in the Hilbert space, they form a $U(1)$ group, and the $U(1)$ here is a global symmetry.

There are four fundamental interactions, strong, electromagnetic, weak, and gravitational, in descending order in strength. In the Standard Model, the electromagnetic and weak interactions are the low-energy realities of a unified interaction — electroweak interaction, and the gravitational interaction is not included.

A permutation of the three colors of the strong interactions will not change the laws of physics, that is the rotation in the color space is an exact symmetry. The three colors of the same flavor of quark form a triplet in the color space, *i.e.* they make a representation of the color group — $SU(3)$. In the list of hadrons, there are several collections of particles that form multiplets. For example, mesons K, π, and η can be identified with a representation of the $SU(3)$ color group [4].

Likewise, the left-handed (e_L, ν_L) or (u_L, d_L) form doublets in the weak isospin space, *i.e.* they form representations of an $SU(2)$ group. The right-handed e_R, u_R, and d_R are singlets in this group, according to the famous violation of parity conservation in weak interaction [5, 6]. The above is also applicable to their counterparts in the second and third generations.

Finally, there is a hypercharge group $U(1)$. The hypercharge Y of a particle can be found from the Gell-Mann–Nishijima formula,

$$Q = I_3 + \frac{1}{2}Y \ , \tag{1.3}$$

where Q is the electric charge and I_3 is the z-component of the isospin of the particle. The fact that a simultaneous phase change associated with hypercharge will not change the laws of physics implies that the hypercharge group $U(1)$ is also a symmetry group of the Standard Model.

To summarize, we have three independent symmetries associated with the Standard Model. The direct product of their corresponding groups, $SU(3)_C \times SU(2)_L \times U(1)_Y$, is the gauge group of the Standard Model.

1.2 Supersymmetry and Supergravity

The Standard Model has been proved to be a successful model in explaining the sub-atomic phenomena, but there is enough evidence that physics beyond the Standard Model exists. Supersymmetry is the most promising approach so far, because of its capability of solving several dilemmas in the Standard Model. We will review supersymmetry in this section.

The most significant disadvantage of the Standard Model may be the gauge hierarchy problem. The electricity neutral part of the Higgs field is a complex scalar H with a classical potential

$$V = m_H^2|H|^2 + \lambda|H|^4 \ , \tag{1.4}$$

where the observed values of m_H^2 and λ are $m_H^2 = -(92.9\ \text{GeV})^2$ and $\lambda = 0.126$. Because the Higgs field couples with all particles, m_H^2 receives large quantum corrections. Assume

there is a coupling Lagrangian term between the Higgs field H and a Dirac fermion f, where for instance, f could be any one of the fermions in the Standard Model[2],

$$-\lambda_f H \bar{f} f \ ,$$

then the 1-loop correction of m_H^2 received from the Dirac fermion is [7],

$$\Delta m_H^2 = -\frac{|\lambda_f|^2}{8\pi^2}\Lambda_{UV}^2 + \cdots \tag{1.5}$$

where Λ_{UV} is the ultraviolet cutoff of the loop integral, and the omitted terms are proportional to m_f^2 and increase at most logarithmically with Λ_{UV}.

Likewise, if the coupling Lagrangian term between the Higgs field and a scalar field S is

$$-\lambda_S |H|^2 |S|^2 \ ,$$

then the 1-loop correction of m_H^2 received from the scalar particle is

$$\Delta m_H^2 = \frac{\lambda_S}{16\pi^2}\left(\Lambda_{UV}^2 - 2m_S^2 \log\frac{\Lambda_{UV}}{m_S} + \cdots\right) \ . \tag{1.6}$$

We interpret Λ_{UV} as the energy where new physics enters, and it is usually taken the value of the Planck scale, $M_P = 1/\sqrt{8\pi G_{\text{Newton}}} = 2.4 \times 10^{18}$ GeV , when quantum gravity plays an important role. However, this will lead to a m_H^2 of 30 orders larger than what is observed. We can either introduce a Λ_{UV} significantly lower than the Planck scale, which results in more problems, or alternatively, we can require the quantum corrections from fermions and bosons neatly cancel. To fulfill this latter idea, we have a simple solution by adding a boson partner to each fermion, and a fermion partner to each boson. Thus, at

[2]Quarks of different colors make their contributions individually.

the cost of doubling the number of elementary particles, the gauge hierarchy problem and several other dilemmas are elegantly solved.

The names of the superparticles are given in the following manner. Firstly, the fermions among the Standard Model elementary particles — quarks and leptons, all have spin 1/2. Their superpartners all have spin 0, which means they are scalar particles. Thus, these particles are named by adding a prefix "s" to the names of their superpartners. For instance, electron's superpartner is called "selectron", standing for "scalar electron". Secondly, the superpartners of the Standard Model gauge bosons and Higgs boson are fermions. They are named by adding a suffix "-ino" to the name of their superpartners. For example, gluon's superpartner is called "gluino".

The Standard Model particles have the same quantum numbers as their superpartners, so that for any SM particle that appears, say, on the Feynman diagram of 1-loop correction of the Higgs boson mass as shown in FIG. 1.2, we can always substitute the Standard Model particle, which is a top quark t in our example, by its superpartner, $\tilde{t}$ here, and the Feynman diagram remains valid.

However, none of these supersymmetric particles has been found yet. This means that supersymmetry is a broken symmetry at energy levels ever achieved by mankind, and that SM particles have different masses than their superpartners.

Supersymmetry is a global symmetry. To localize them, *i.e.*, to allow the group elements to vary with the space-time coordinates, we need a spin 3/2 field and its superpartner with spin 2 [8]. A graviton, the quantum of the gravitational field, is the spin 2 field needed by the localization of supersymmetry. Its superpartner — gravitino, is therefore identified with the spin 3/2 field. So supergravity is local supersymmetry, or supersymmetry with gravity.

1.3 Grand Unified Theory

1.3.1 Motivation

The Standard Model is very successful in explaining most properties of the elementary particles found to date, despite some imperfections. Firstly, its gauge group $SU(3) \times SU(2) \times U(1)$ has three different couplings. There are also many parameters to be adjusted, and the fermions are assigned by convenience, not by principle [9]. Intuitively, a "larger" group with a single gauge coupling and fewer free adjustable parameters would be preferred.

1.3.2 Georgi-Glashow $SU(5)$

An early attempt to unify the strong and electroweak interactions is the Georgi-Glashow $SU(5)$ Model [10]. Because the rank of the gauge group $SU(3) \times SU(2) \times U(1)$ is 4, the minimal simple Lie group containing it is $SU(5)$, whose rank is also 4. So $SU(5)$ is undoubtedly the first Lie group on which one would try to build the grand unified theory (GUT).

The calculation of anomaly [9] shows that the anomaly-free $SU(5)$ representation is $\bar{\mathbf{5}} + \mathbf{10}$. Recall that there are 15 constituents in any of the three generations of fermions, Taking the first generation as an example, they include one electron, one positron, one neutrino, three up quarks (one in each of the three colors) and three up anti-quarks, and three down quarks (likewise) and three down anti-quarks. If we use each of these dimensions to represent the quantum numbers of these fermions, the $\bar{\mathbf{5}} + \mathbf{10}$ representation fits everything in perfectly.

The $\bar{\mathbf{5}}$-dimensional representation is usually chosen to represent the right-handed fermions. For convenience we write them in the $\bar{\mathbf{5}}$ representation of their left-handed conjugate states so that all particles written down are left-handed,

$$\psi = \begin{pmatrix} d_1^c \\ d_2^c \\ d_3^c \\ e \\ \nu \end{pmatrix}_L \quad ; \tag{1.7}$$

and $\mathbf{10}$-dimensional representation for left-handed fermions,

$$\chi = \begin{pmatrix} 0 & u_3^c & -u_2^c & u_1 & d_1 \\ & 0 & u_1^c & u_2 & d_2 \\ & & 0 & u_3 & d_3 \\ & & & 0 & e^+ \\ & & & & 0 \end{pmatrix}_L \quad . \tag{1.8}$$

For bosons, the matrix form of the generators are shown in Appendix B.

However, the Georgi-Glashow $SU(5)$ model, along with other GUTs, predicts that the baryon number is not conserved, thus protons can decay, which has never been observed. The 2012 Super-Kamiokande result [11] shows that the half-life of proton is at least

$$\tau_p \sim 10^{34} \text{ yrs} \tag{1.9}$$

And with larger instruments being adapted, the experimental constraints will likely increase. This motivates us to look for other ways to the objective of unification. One of these models — the flipped $SU(5)$ is paid special attention next.

1.4 The Flipped $SU(5)$ Model

Flipped $SU(5)$ [12, 13, 14] is an alternative symmetry breaking of $SO(10)$ grand unified model into $SU(5) \times U(1)_X$, which is a different subgroup of $SO(10)$ than the Georgi-

Glashow $SU(5)$. The breaking chain of flipped $SU(5)$ is

$$
\begin{array}{c}
SO(10) \\
\downarrow \\
SU(5) \times U(1)_X \\
\downarrow \\
SU(3)_C \times SU(2)_L \times U(1)_Y \\
\downarrow \\
SU(3)_C \times U(1)_{\rm em}
\end{array}
$$

in contrast to that of Georgi-Glashow $SU(5)$,

$$
\begin{array}{c}
SO(10) \\
\downarrow \\
SU(5) \\
\downarrow \\
SU(3)_C \times SU(2)_L \times U(1)_Y \\
\downarrow \\
SU(3)_C \times U(1)_{\rm em}
\end{array}
$$

The $\mathbf{5}$-dimensional right-handed fermion representation of flipped $SU(5)$ is

$$\bar{f} = \begin{pmatrix} u_1 \\ u_2 \\ u_3 \\ \nu^c \\ e^+ \end{pmatrix}_R \quad ; \tag{1.10}$$

and $\mathbf{10}$-dimensional left-handed,

$$F = \begin{pmatrix} 0 & d_3^c & -d_2^c & d_1 & u_1 \\ & 0 & d_1^c & d_2 & u_2 \\ & & 0 & d_3 & u_3 \\ & & & 0 & \nu^c \\ & & & & 0 \end{pmatrix}_L \quad , \tag{1.11}$$

in addition to a $\mathbf{1}$-dimensional singlet of electron,

$$l^c = (e^c)_L \; . \tag{1.12}$$

In contrast to the representation of Georgi-Glashow $SU(5)$ in Eqs. 1.7 and 1.8, it can be found that the difference is that the up-type quarks and down-type quarks are interchanged, and the right-handed neutrino is in the place of the positron, making the right-handed neutrino mandatory[3]. This is the origin of "flipped" in the name of the model.

For the minimal flipped $SU(5)$ model, the generator $U(1)_{Y'}$ in $SU(5)$ is defined by

[3]The existence of the right-handed neutrino can be inferred from the observation of neutrino oscillation, but is not included in neither the Standard Model or the Georgi-Glashow $SU(5)$.

$$T_{\mathrm{U}(1)_{\mathrm{Y}'}} = \mathrm{diag}\left(-\frac{1}{3}, -\frac{1}{3}, -\frac{1}{3}, \frac{1}{2}, \frac{1}{2}\right). \tag{1.13}$$

and the hypercharge is

$$Q_Y = \frac{1}{5}\left(Q_X - Q_{Y'}\right). \tag{1.14}$$

We may rewrite the three families of SM particles given in Eqs. 1.10-1.12 in a more compact form,

$$F_i = (Q_i, D_i^c, N_i^c)\ ,\ \overline{f}_i = (U_i^c, L_i)\ ,\ \bar{l}_i = E_i^c\ , \tag{1.15}$$

where, Q_i and L_i are the superfields of the left-handed quark and lepton doublets, i.e. $\begin{pmatrix} u \\ d \end{pmatrix}_L$ and $\begin{pmatrix} e \\ \mu \end{pmatrix}_L$, respectively; U_i^c, D_i^c, E_i^c and N_i^c are the CP conjugated superfields for the right-handed up-type quarks, down-type quarks, leptons and neutrinos, i.e. $\begin{pmatrix} u_1^c \\ u_2^c \\ u_3^c \end{pmatrix}_L$, $\begin{pmatrix} d_1^c \\ d_2^c \\ d_3^c \end{pmatrix}_L$, (e_L^c), and (μ_L^c) respectively. Massive right-handed neutrinos can be generated by introducing three SM singlets. The quantum numbers of the three families of the Standard Model fermions under $SU(5) \times U(1)_X$ are,

$$F_i = (\mathbf{10}, \mathbf{1}) \ , \ \overline{f}_i = (\bar{\mathbf{5}}, -\mathbf{3}) \ , \ \bar{l}_i = (\mathbf{1}, \mathbf{5}), \tag{1.16}$$

where $i = 1, 2, 3$. In our convention, the normalization factor for $U(1)_X$ charges is $\frac{1}{2\sqrt{10}}$.

To break the GUT and electroweak gauge symmetries, we introduce two pairs of Higgs representations,

$$\begin{aligned} H = (\mathbf{10}, \mathbf{1}) \quad &, \quad \overline{H} = (\overline{\mathbf{10}}, -\mathbf{1}) \ , \\ h = (\mathbf{5}, -\mathbf{2}) \quad &, \quad \overline{h} = (\bar{\mathbf{5}}, \mathbf{2}) \ . \end{aligned} \tag{1.17}$$

The states in the H multiplet are put in the same order as in the F multiplet, as can be seen from the explicit form below,

$$H = (Q_H, D_H^c, N_H^c) \ , \ \overline{H} = (\overline{Q}_{\overline{H}}, \overline{D}_{\overline{H}}^c \ , \overline{N}_{\overline{H}}^c) \ , \tag{1.18}$$

$$h = (D_h, D_h, D_h, H_d) \ , \ \overline{h} = (\overline{D}_{\overline{h}}, \overline{D}_{\overline{h}}, \overline{D}_{\overline{h}}, H_u) \ , \tag{1.19}$$

where H_d and H_u are one pair of Higgs doublets in the MSSM. Also needed is an SM singlet Φ.

The $SU(5) \times U(1)_X$ gauge symmetry can be broken down to the $SU(3)_C \times SU(2)_L \times U(1)_Y$ gauge symmetry by the following Higgs superpotential at the GUT scale

$$W_{\rm GUT} = \lambda_1 HHh + \lambda_2 \overline{HHh} + \Phi(\overline{H}H - M_{\rm H}^2)\ . \tag{1.20}$$

We can always rotate the only F-flat and D-flat direction along the N_H^c and $\overline{N}_{\overline{H}}^c$ directions, and obtain $\langle N_H^c \rangle = \langle \overline{N}_{\overline{H}}^c \rangle = M_{\rm H}$. Particles acquire masses by eating superfields H and $\overline{H}$ via the SUSY Higgs mechanism, except D_H^c and $\overline{D}_{\overline{H}}^c$, who acquire masses $2\lambda_1 \langle N_H^c \rangle$ and $2\lambda_2 \langle \overline{N}_{\overline{H}}^c \rangle$ by being coupled by the superpotential terms $\lambda_1 HHh$ and $\lambda_2 \overline{HHh}$ with D_h and $\overline{D}_{\overline{h}}$, respectively.

1.5 The No-scale $\mathcal{F}$-$SU(5)$ Model

Flipped $SU(5)$ can be built from F-theory and free fermionic string models [15, 16, 17]. In order to obtain the string-scale gauge coupling unification, two sets of vector-like particles around TeV scale are introduced, as will be discussed soon. We call it $\mathcal{F}$-$SU(5)$, where the $\mathcal{F}$ represents both *F-theory* and *free fermionic*. Next we will focus on the no-scale $\mathcal{F}$-$SU(5)$ model.

In order to fulfill string-scale gauge coupling unification [15, 16, 17], the following vector-like particles (flippons) are introduce at the TeV scale,

$$XF = (\mathbf{10}, \mathbf{1}) \quad , \quad \overline{XF} = (\overline{\mathbf{10}}, -\mathbf{1})\ , \tag{1.21}$$

$$Xl = (\mathbf{1}, -\mathbf{5}) \quad , \quad \overline{Xl} = (\mathbf{1}, \mathbf{5})\ , \tag{1.22}$$

which can be decomposed under the SM gauge symmetry. Thus we have the following particle content,

$$XF = (XQ, XD^c, XN^c) \quad , \quad \overline{XF} = (XQ^c, XD, XN) \, , \tag{1.23}$$

$$Xl = XE \quad , \quad \overline{Xl} = XE^c \, . \tag{1.24}$$

whose quantum numbers under the $SU(3)_C \times SU(2)_L \times U(1)_Y$ gauge symmetry are

$$XQ = \left(\mathbf{3}, \mathbf{2}, \frac{\mathbf{1}}{\mathbf{6}}\right) \quad , \quad XQ^c = \left(\bar{\mathbf{3}}, \mathbf{2}, -\frac{\mathbf{1}}{\mathbf{6}}\right) , \tag{1.25}$$

$$XD = \left(\mathbf{3}, \mathbf{1}, -\frac{\mathbf{1}}{\mathbf{3}}\right) \quad , \quad XD^c = \left(\bar{\mathbf{3}}, \mathbf{1}, \frac{\mathbf{1}}{\mathbf{3}}\right) , \tag{1.26}$$

$$XN = (\mathbf{1}, \mathbf{1}, \mathbf{0}) \quad , \quad XN^c = (\mathbf{1}, \mathbf{1}, \mathbf{0}) \, , \tag{1.27}$$

$$XE = (\mathbf{1}, \mathbf{1}, -\mathbf{1}) \quad , \quad XE^c = (\mathbf{1}, \mathbf{1}, \mathbf{1}) \, . \tag{1.28}$$

A major drawback of the Georgi-Glashow $SU(5)$, the doublet-triplet splitting problem, can be addressed by $\mathcal{F}$-$SU(5)$ naturally via the missing partner mechanism [14].

Because no supersymmetric particles has been found in any experiments performed so far, supersymmetry must be broken, and the breaking must occur at or near the TeV scale due to the mass difference between SM particles and SUSY particles.

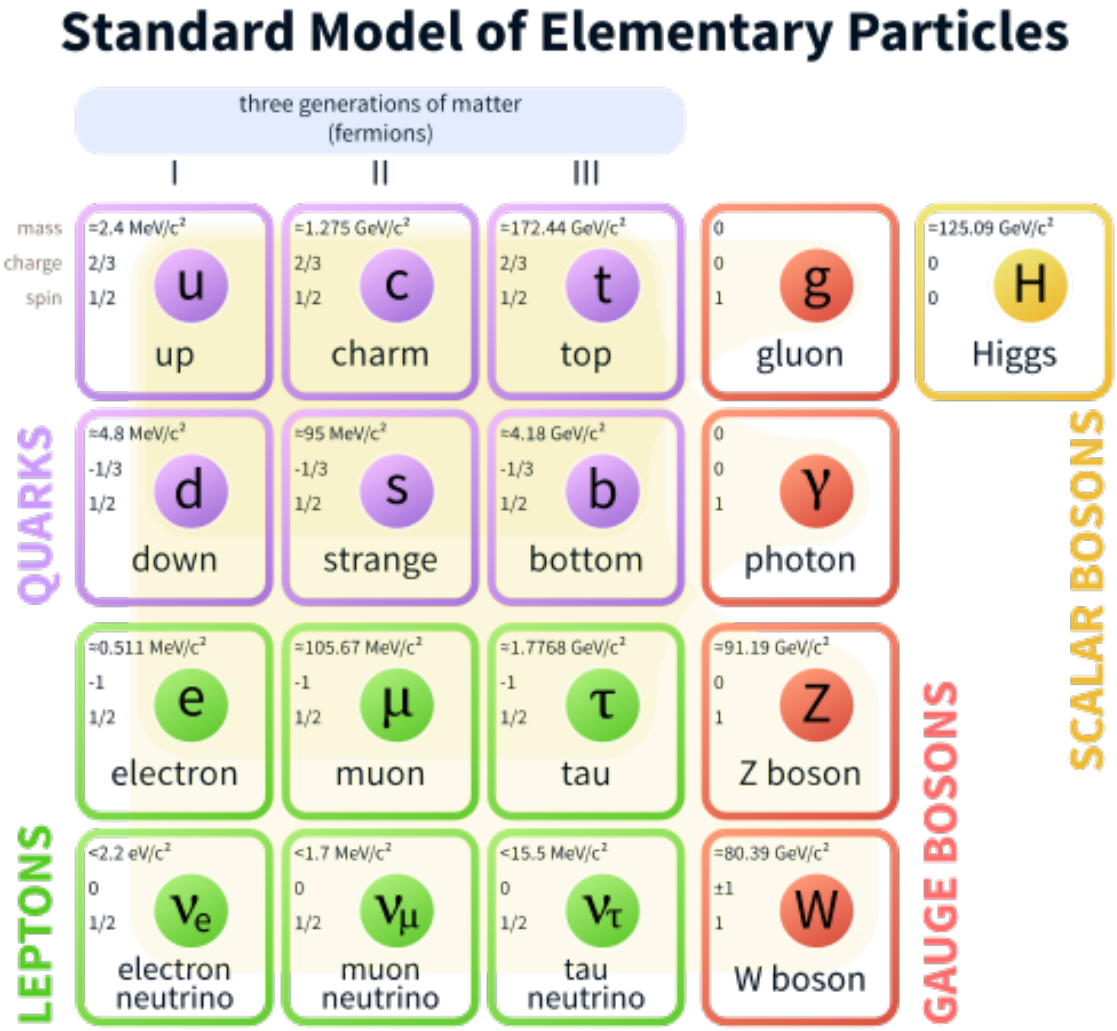

Figure 1.1: Summary of Elementary Particles. Reprinted from [1].

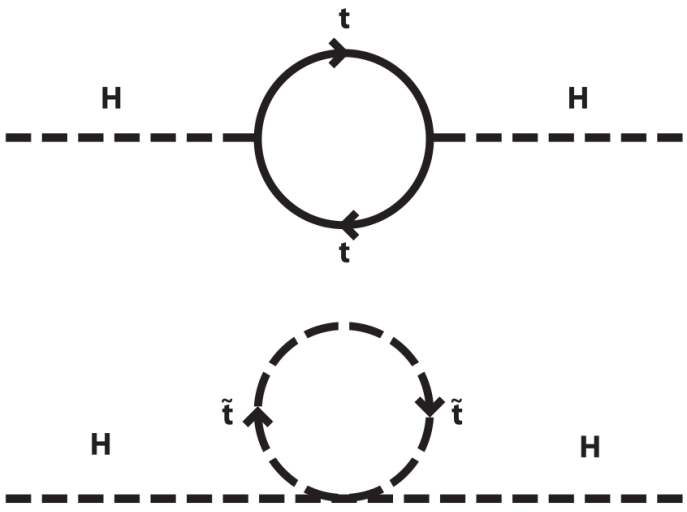

Figure 1.2: One-loop corrections to the Higgs mass from top quark and stop squark. Reprinted from [2].

2. NUMERICAL CALCULATIONS

We begin this chapter by introducing the traditional methodology of studying the $\mathcal{F}$-$SU(5)$ model. We then introduce the new methodology adopted, the general No-Scale boundary conditions. We conclude this chapter by presenting the numerical results of the calculations.

2.1 Strict No-Scale Boundary Conditions

In the traditional No-Scale boundary conditions [18, 19, 20, 21, 22], a simple Kähler potential

$$K = -3 \ln \left(T + \overline{T} - \frac{1}{3} \sum_i \overline{\Phi}_i \Phi_i \right)$$

is used to solve the cosmological flatness problem. This implies the strict No-Scale SUGRA boundary condition $M_0 = A = B_\mu = 0$ at the unification scale $M_{\mathcal{F}}$. The vector-like particle (flippon) mass scale M_V, top quark mass m_t, and low energy ratio of Higgs vacuum expectation values (VEVs) $\tan\beta$ are expressed as a function of the gaugino mass $M_{1/2}$. So $M_{1/2}$ remains the only free parameter, giving a One-Parameter Model (OPM).

Although the parameter space is highly constrained, the phenomenology derived from the model is of interest.

The strict No-Scale boundary conditions result in a massive vector-like flippon mass of $M_V \sim 23 - 50$ TeV, largely beyond the reach of the current or future phases of the LHC running.

2.2 General No-Scale boundary conditions

In order to exploit the whole No-Scale $\mathcal{F}$-$SU(5)$ parameter space beyond the 1-dimensional parameter space set by the strict No-Scale boundary conditions $M_0 = A_0 = B_\mu = 0$, we relax the tight constraints by allowing the scalar mass M_0, the trilinear soft term A_0, and

the bilinear term B_μ to be non-zero in general.

The lower and upper limits of each parameter are given in Table 2.1, i.e. each of the parameters characterizing the SUSY breaking soft term, in addition to the vector-like flippon mass decoupling scale M_V and top quark mass m_t, is assigned a value within its range independently. The most recent LHC constraints on vector-like T and B quarks [23] bounds (XQ, XQ^c) vector-like flippons at about 855 GeV and (XD, XD^c) vector-like flippons about 735 GeV from below. Thus the lower limit of vector-like flippon mass M_V is set to 855 GeV. The range of m_t is taken to allow sufficient range around the world average [24]. Also taken into account is that the M_0 and A_0 are allowed to be assigned a value freely, and only the consistency of their phenomenology and the experimental results determines their viability. However, B_μ is not constrained in this study.

Table 2.1: Parameter space used in the numerical calculations of the General No-scale $\mathcal{F}$-$SU(5)$ boundary condition.

	Lower Limit	Upper Limit
$M_{1/2}$	100 GeV	$5,000$ GeV
M_0	100 GeV	$5,000$ GeV
A_0	$-5,000$ GeV	$5,000$ GeV
$\tan\beta$	2	65
M_V	855 GeV	$100,000$ GeV
m_t	171 GeV	175 GeV

The $\mathcal{F}$-$SU(5)$ mSUGRA/CMSSM high-energy boundary conditions $M_{1/2}$, M_0, and A_0 are applied at the ultimate unification scale $M_{\mathcal{F}} \simeq 5 \times 10^{17}$GeV, the scale of the ultimate stage of unification in $\mathcal{F}$-$SU(5)$.This is in contrast to the minimal supersymmetric standard model (MSSM) in which these boundary conditions are taken at the GUT scale $\sim 10^{16}$ GeV.

It is expected that the mSUGRA/CMSSM boundary conditions will allow the SUSY spectrum to be light, and the Higgs boson mass to lifted to the experimental measured range by the vector-like flippon Yukawa coupling to the Higgs boson. Flexible SUSY breaking parameters can also allow a more flexible flippon mass scale M_V. They altogether provide a more testable SUSY spectrum.

To summarize, in this study the applied SUSY soft terms are $M_{1/2}$, M_0, and A_0, which are the primary components of the mSUGRA/CMSSM SUSY breaking terms.

Another alternative is to involve the D-brane inspired soft terms, which have the following parameters:$M_1, M_5, M_{\tilde{Q}} = M_{\tilde{D}^c}, M_{\tilde{L}} = M_{\tilde{U}^c}, M_{\tilde{E}^c}, M_H, A_t, A_b, A_\tau, \tan\beta$, and the sign of μ. These come directly from the $\mathcal{F}$-$SU(5)$ representations in Eqs. 1.10 - 1.12.

2.3 Sampling Process

A total of 24 million points are sampled in random scans applying these mSUGRA/ CMSSM boundary conditions at the $M_{\mathcal{F}}$ scale, and 40 million points for the D-brane inspired boundary conditions. `MicrOMEGAs 2.1` [25] is used to calculate the SUSY mass spectra, relic density, rare decay processes, and direct dark matter detection cross-sections, utilizing a proprietary modification of the `SuSpect` code-base [26] to run flippon and General No-Scale $\mathcal{F}$-$SU(5)$ enhanced RGEs.

3. DATA ANALYSIS*

We begin this chapter by presenting the currently collected results from high-energy physics experiments. We then present the procedure of processing the numerical simulations. We conclude this chapter with the phenomenology.

3.1 Constraints imposed by experimental results

The Large Hadron Collider (LHC) is built to explore multi-TeV physics. It is hoped that the LHC could find the evidence of the existence of the SUSY particles. However, the first phase of LHC since 2009 has not yet found any conclusive signals that belong to SUSY particles.

Despite the null results in SUSY search, the LHC has successfully discovered the evidence of the Higgs boson particle, with a mass of $m_h = 125.09$ GeV [27, 28]. For the purpose of generating the 1-loop and 2-loop contributions to the Higgs boson mass m_h due to the large top Yukawa coupling, the light stop mass $m_{\tilde{t}_1}$ is required to be heavy in minimalistic models, such as minimal Supergravity (mSUGRA) and Constrained Minimal Supersymmetric Standard Model (CMSSM) that we are looking into.

The viable parameter space is required to be consistent with both the WMAP 9-year [29] and the 2015 Planck [30] relic density measurements. They impose upper limits of

$$\Omega h^2 \leq 0.1300 \, ,$$

where we allow the inclusion of multi-component dark matter beyond the neutralino.

The most recent LHC gluino search [31] sets a strict lower limit on the gluino mass in

*Reprinted with permission from "General No-Scale Supergravity: An $\mathcal{F}$-$SU(5)$ tale" by D. Hu, T. Li, A. Lux, J. A. Maxin, and D. V. Nanopoulos, 2017. *Physics Letters*, B771, 264-270. Copyright [2017] by Elsevier.

the model space of

$$M_{\tilde{g}} \geq 1.9 \text{ TeV} .$$

A lower limit of

$$M_{\tilde{t}_1} \geq 900 \text{ GeV}$$

on the light stop mass [31] is also imposed.

The light Higgs boson mass boundary is set to

$$123 \text{ GeV} \leq m_h \leq 128 \text{ GeV}$$

to allow for at least 2σ experimental uncertainty floating around the experimental central value of

$$m_h = 125.09 \text{ GeV} .$$

The lower and upper bounds correspond to maximal and minimal flippon Yukawa couplings, respectively.

The branching ratio of the rare b-quark decay [32] is applied as a constraint

$$Br(b \to s\gamma) = (3.43 \pm 0.21^{stat} \pm 0.24^{th} \pm 0.07^{sys}) \times 10^{-4} ,$$

as well as the branching ratio of the rare B-meson decay to a dimuon [33]

$$Br(B_s^0 \to \mu^+\mu^-) = (2.9 \pm 0.7 \pm 0.29^{th}) \times 10^{-9} .$$

The 3σ intervals around the SM value and experimental measurement of the SUSY

contribution to the anomalous magnetic moment of the muon [34] is

$$-1.2 \times 10^{-10} \leq \Delta a_\mu \leq 51.0 \times 10^{-10} \, .$$

COUPP Collaboration [35] and XENON100 Collaboration [36] also impose limits on the proton spin-dependent cross-sections.

So far, all constraints except those on the spin-independent (SI) cross-sections for neutralino-nucleus interactions from the Dark Matter detection are applied on the sampled points. We find that M_{H^0} and M_{LSP} of the points within all these limits are uncorrelated, and the parameter space is not separable.

3.1.1 Spin-independent cross-sections

The August 2016 result from Large Underground Xenon (LUX) experiment [37] and earlier Particle AND Astrophysical Xenon detector (PandaX)-II experiment [38] impose upper limits on spin-independent cross-sections for neutralino-nucleus interactions. In order to be consistent with these results and to account for multi-component dark matter, we re-scale the SI cross-section of each sampled points by the ratio of its relic densities, numerically calculated with its parameter combination, to 0.1138, an average of WMAP 9-year [29] and 2015 Planck [30] relic density measurements,

$$\sigma_{\text{SI(SD)}}^{\text{re-scaled}} = \sigma_{\text{SI(SD)}} \frac{\Omega h^2}{0.1138} \, , \tag{3.1}$$

and then exclude those points with excessive re-scaled SI cross-sections in accordance with the DM experiments. The viable points then clearly display gaps dividing them into multiple categories. Fig. 3.1 illustrates the viable parameter space under the LUX and PandaX-II WIMP-nucleon spin-independent cross-section constraints. The bino LSP, Higgs Funnel, Higgsino LSP and the Mixed scenarios are annotated as different regions on

the plot. The spin-independent cross-sections have been rescaled according to Eq. (3.1). The empty regions between the viable regions are excluded by the constraints on the gluino mass, the light Higgs boson mass, and the relic density. The gray region above the LUX and PandaX-II is excluded due to excessive SI cross-sections, but they indeed satisfy the constraints by all the other experiments. The red curve on Fig. 3.1 is the upper bound on coherent neutrino scattering from atmospheric neutrinos and the diffuse supernova neutrino background (DSNB), which is considered as the lower limit on the direct probe of WIMP-nucleon scattering. The viable stau coannihilation region is above the neutrino scattering limits.

3.2 Phenomenological Analysis for mSUGRA/CMSSM Boundary Conditions

The phenomenological analysis will be conducted in two aspects. We begin by inspecting the parameter space spanned by the mSUGRA/CMSSM soft supersymmetry breaking terms, and find the intrinsic logic to investigate the dark matter composition. Then we study the observable signatures of each of the regions of special interest, on the purpose that the model could be tested at a higher energy.

3.2.1 Classification of the viable parameter space

The viable parameter space can be divided into five categories based on LSP composition, as shown in TABLE 3.1. Each LSP is nearly all bino (Stau and Higgs Funnel) or all higgsino (Higgsino and Mixed).

The five dark matter scenarios can be characterized by the particles states emanating from the SUSY cascade decay,

1. Bino LSP with stau coannihilation and $M_{\tilde{t}_1} < M_{\tilde{g}}$;

2. Bino LSP with stau coannihilation and $M_{\tilde{g}} < M_{\tilde{t}_1}$;

3. Higgs Funnel, defined by $M_{H^0} \simeq 2M_{\tilde{\chi}_1^0}$;

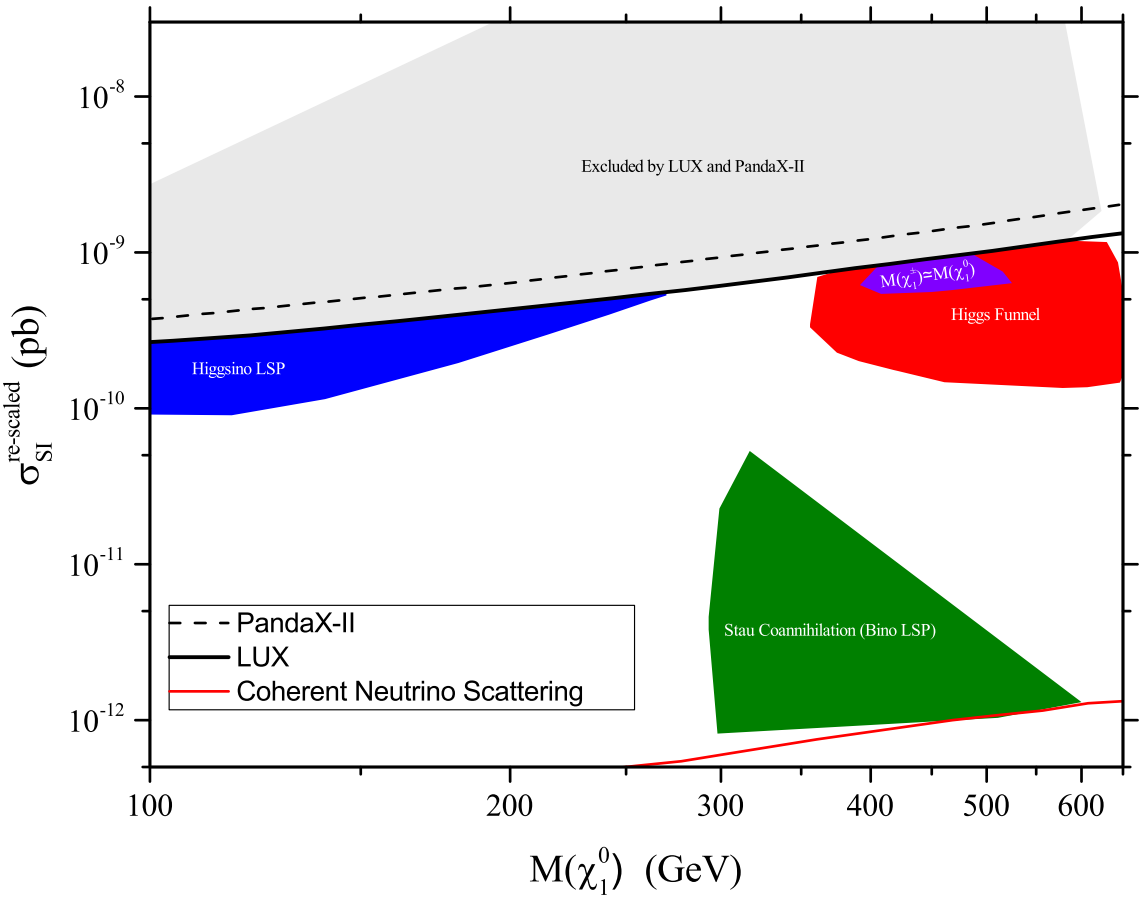

Figure 3.1: Depiction of the LUX and PandaX-II spin-independent cross-section constraints applied to the General No-Scale $\mathcal{F}$-$SU(5)$ viable parameter space.

.

Table 3.1: General No-scale $\mathcal{F}$-$SU(5)$ lightest supersymmetric particle (LSP) composition for the five dark matter regions studied. The one-parameter version of the No-scale $\mathcal{F}$-$SU(5)$ model is listed for comparison.

Scenario	LSP Composition
Stau ($M_{\tilde{t}_1} < M_{\tilde{g}}$)	100% bino
Stau ($M_{\tilde{g}} < M_{\tilde{t}_1}$)	100% bino
Higgs Funnel	99% bino
Higgsino	100% higgsino
Mixed	98% higgsino
One-parameter Model	100% bino

4. Higgsino LSP;

5. Mixture of Higgs Funnel and Higgsino LSP.

Categories 2 - 5 posses the typical mSUGRA/CMSSM SUSY spectrum mass ordering of $M_{\tilde{g}} < M_{\tilde{t}_1} < M_{\tilde{q}}$, while category 1 and the one-parameter $\mathcal{F}$-$SU(5)$ generate a unique mass ordering of $M_{\tilde{t}_1} < M_{\tilde{g}} < M_{\tilde{q}}$. They all contain neutralino relic density less than the observed value, and support multi-component dark matter.

TABLEs 3.3 - 3.7 show a total of twenty-three benchmark points picked from each category.

FIG. 3.2 displays that a branch of points are surrounding the function graph of $M_{H^0} = 2M_{\text{LSP}}$, i.e. the Higgs Funnel scenario represented by the benchmark spectra shown in TABLE 3.5. Its density map, FIG. 3.3, depicts that the Higgs Funnel consists of a significant number of points generated. Our statistics shows that more than 70% of all viable points belong to this category.

FIG. 3.4 displays that another branch of points, other than those referred in FIG. 3.2, ranging from 100 GeV to 270 GeV in M_{LSP}, are tightly attached to the straight line given by $M_{\tilde{\chi}_1^\pm} = M_{\text{LSP}}$, i.e. the Higgsino LSP scenario. Sample benchmark points of this category are listed in TABLE 3.6. FIG. 3.5 is the density map of FIG. 3.4. About 25% of all viable points are in this region.

There are a small amount of points classified as Higgs Funnel scenario staying near the straight line in FIG. 3.4 as well. They are colored in purple in FIG. 3.4. This region is of interest because they are the overlap of two scenarios. We list the benchmark points from this special region as Mixed in TABLE 3.7.

All points left behind by the previous scenarios are found to be sticking to the function graph of $M_{\tilde{\tau}_1} = M_{\text{LSP}}$, i.e. the stau co-annihilation scenario, as displayed in Fig. 3.6. We find that it has no overlap with previous scenarios. The benchmark points taken here are

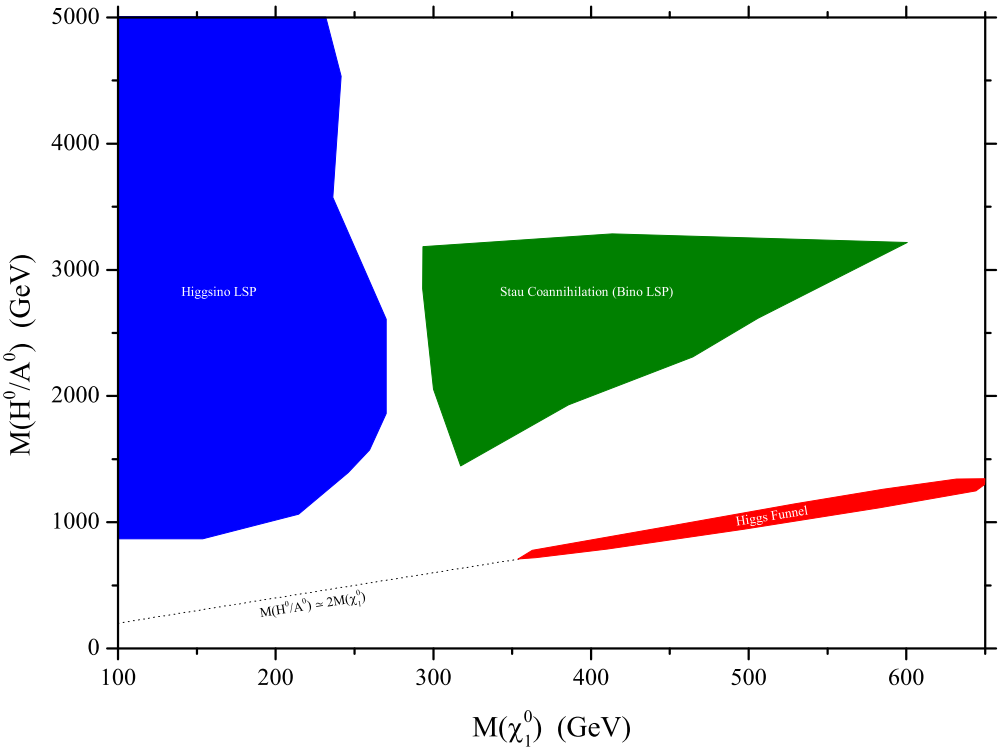

Figure 3.2: All viable dark matter regions with their respective M_{H^0/A^0} and M_{LSP}. The Higgs Funnel defined by $M_{H^0/A^0} \simeq 2M_{\text{LSP}}$ is represented by the dashed line.

.

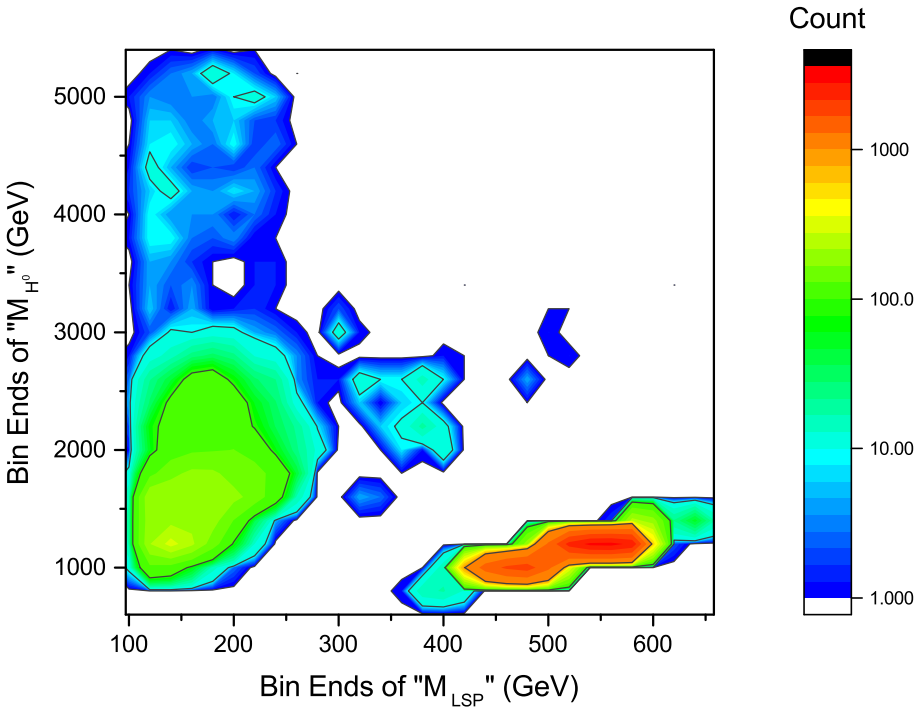

Figure 3.3: Depiction of relative point density of FIG. 3.2.

.

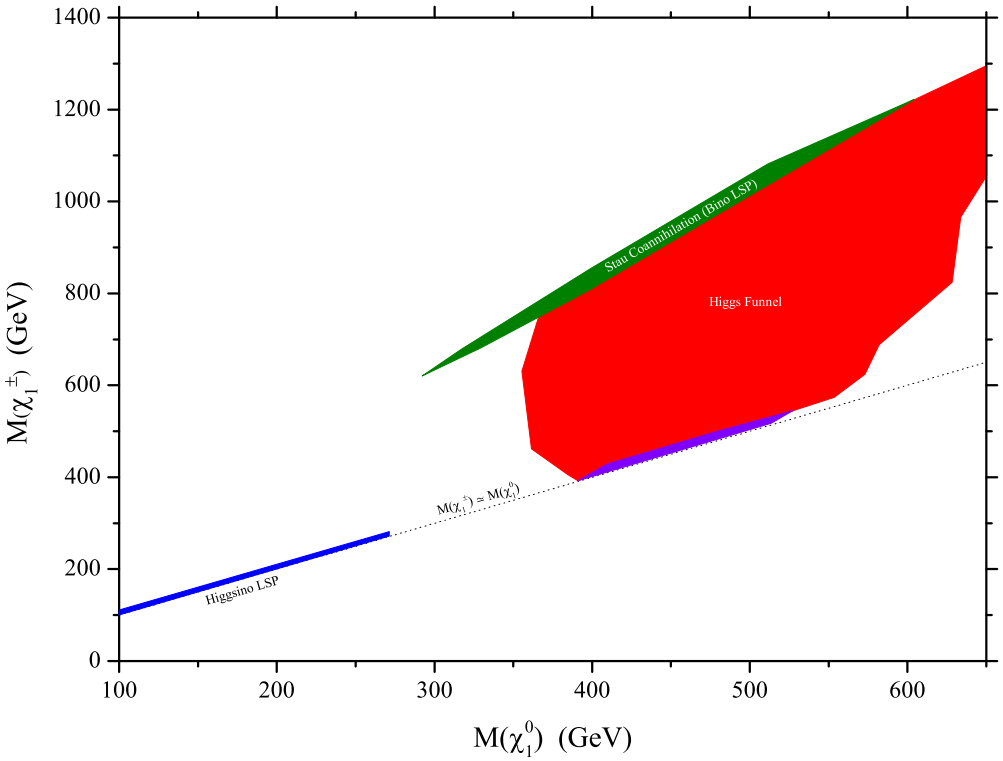

Figure 3.4: All viable dark matter regions with respect to $M_{\tilde{\chi}_1^\pm}$ and M_{LSP}. The highlighted portion of Higgs Funnel satisfies $M_{\tilde{\chi}_1^\pm} \simeq M_{\text{LSP}}$, represented by the dashed line, as well as the Higgsino LSP scenario.

.

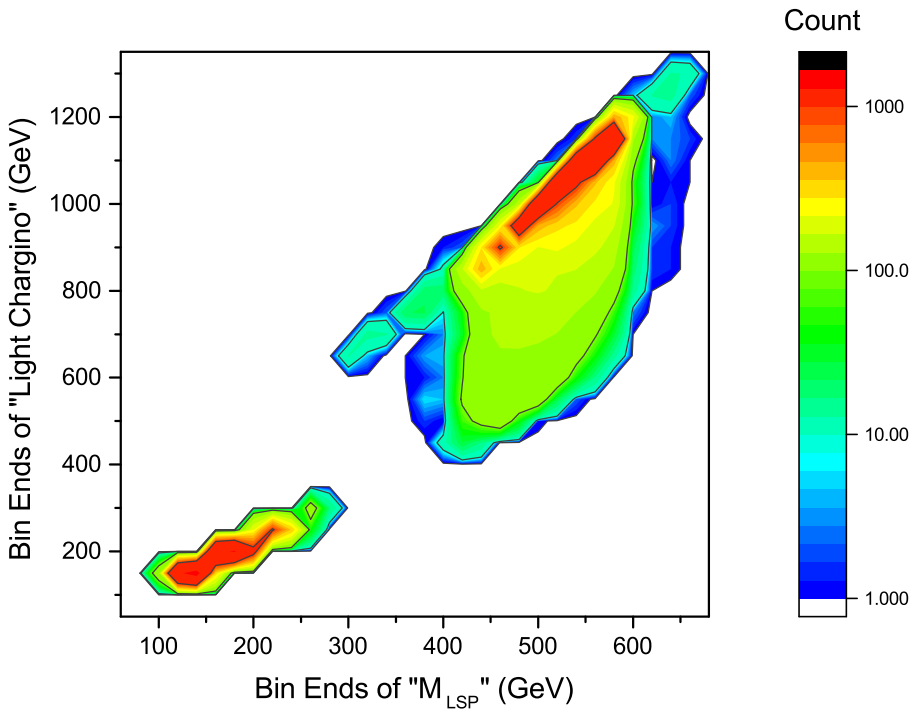

Figure 3.5: Depiction of relative point density of FIG. 3.4.

.

listed as Stau in Table 3.3 - 3.4. Fig. 3.7 is the density map of Fig. 3.6.

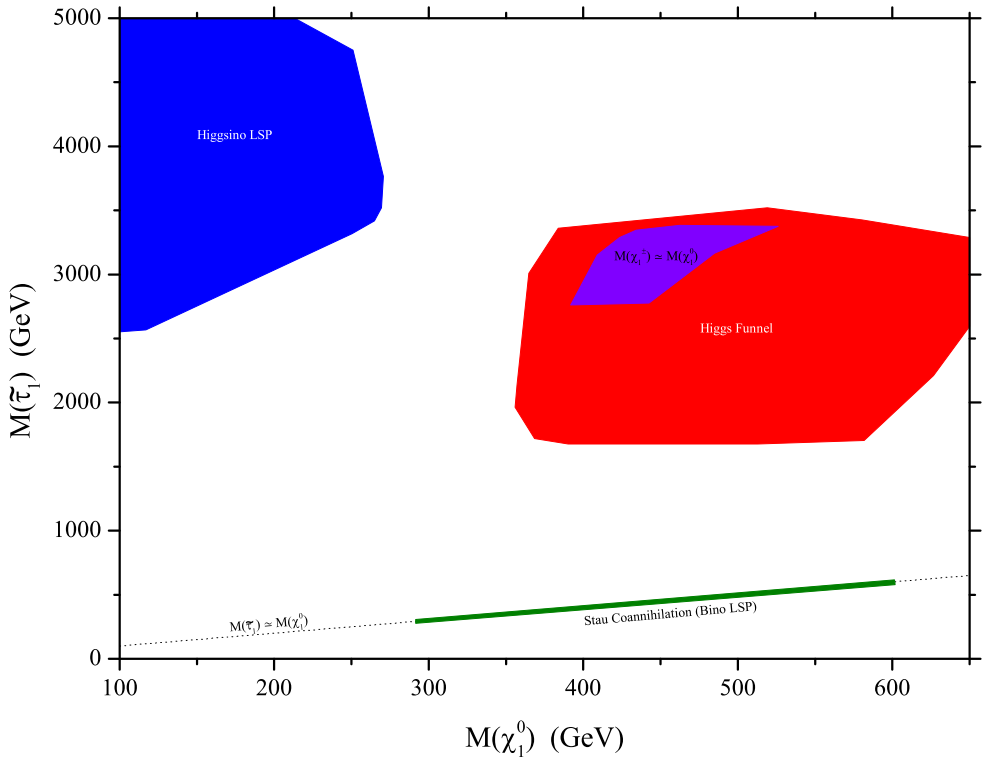

Figure 3.6: All viable dark matter regions with respect to $M_{\tilde{\tau}_1}$ and $M_{\rm LSP}$. The Stau Coannihilation defined by $M_{\tilde{\tau}_1} \simeq M_{\rm LSP}$ is represented by the dashed line.

.

3.2.2 Observable signatures

To test these models, we need to identify observable signatures. The decay modes of selected benchmark points of each scenario are calculated with `SUSY-HIT` [39] software package, and organized by a self-made program.

The leading cascade decay channels of each dark matter region are listed in TABLE 3.2. The difference in the gluino branching ratio between Higgsino LSP and Mixed scenarios is negligible, so they are grouped together.

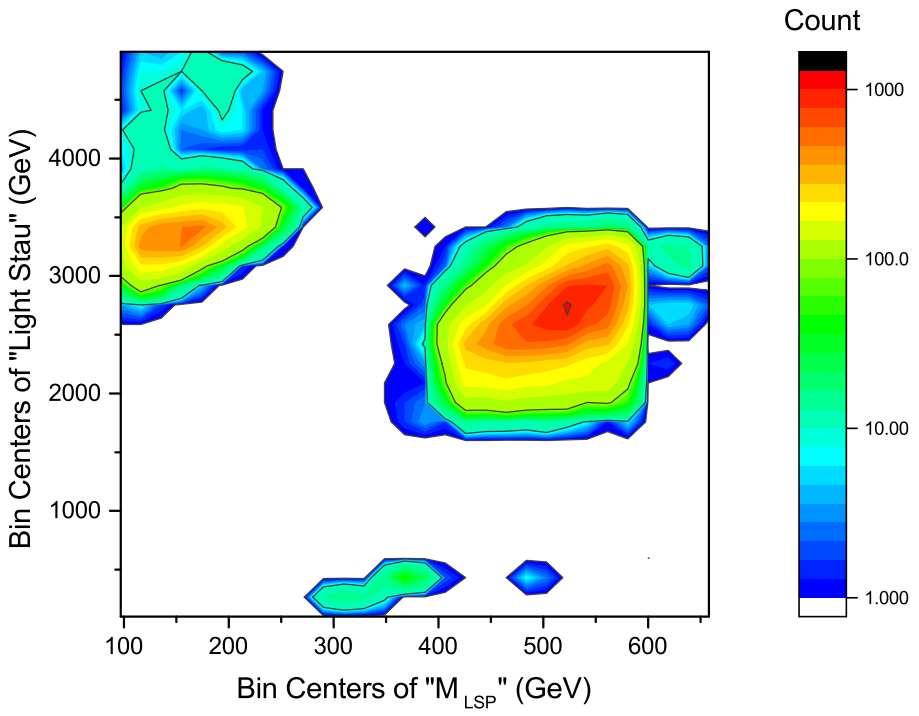

Figure 3.7: Depiction of relative point density of FIG. 3.6.

.

Table 3.2: General No-Scale $\mathcal{F}$-$SU(5)$ leading cascade decay channels for the five different dark matter regions studied in this work. The BR column represents the branching ratio.

Model	BR	Decay Mode
Stau ($M_{\widetilde{t}_1} < M_{\widetilde{g}}$)	0.62	$\widetilde{g} \to t\bar{t} + \widetilde{\chi}_1^0$
Stau ($M_{\widetilde{t}_1} < M_{\widetilde{g}}$)	0.11	$\widetilde{g} \to tb + \tau + \nu_\tau + \widetilde{\chi}_1^0$
Stau ($M_{\widetilde{g}} < M_{\widetilde{t}_1}$)	0.31	$\widetilde{g} \to t\bar{t} + \widetilde{\chi}_1^0$
Stau ($M_{\widetilde{g}} < M_{\widetilde{t}_1}$)	0.19	$\widetilde{g} \to tb + \tau + \nu_\tau + \widetilde{\chi}_1^0$
Stau ($M_{\widetilde{g}} < M_{\widetilde{t}_1}$)	0.19	$\widetilde{g} \to q\bar{q} + \tau + \nu_\tau + \widetilde{\chi}_1^0$
Stau ($M_{\widetilde{g}} < M_{\widetilde{t}_1}$)	0.15	$\widetilde{g} \to q\bar{q} + \tau^+\tau^- + \widetilde{\chi}_1^0$
Higgs Funnel	0.30	$\widetilde{g} \to tb + W + \widetilde{\chi}_1^0$
Higgs Funnel	0.11	$\widetilde{g} \to t\bar{t} + Z + \widetilde{\chi}_1^0$
Higgs Funnel	0.09	$\widetilde{g} \to t\bar{t} + h + \widetilde{\chi}_1^0$
Higgsino/Mixed	0.28	$\widetilde{g} \to tb + q\bar{q} + \widetilde{\chi}_1^0$
Higgsino/Mixed	0.12	$\widetilde{g} \to t\bar{t} + \widetilde{\chi}_1^0$

In models whose gluino is heavier than light stop, the decay options of gluino is mostly concentrated at $\widetilde{g} \to t\bar{t} + \widetilde{\chi}_1^0$. Otherwise, there are several decay channels of gluino, but none of them are dominant. Thus, the $t\bar{t}$ channel may be utilized as an indicator to differentiate these regions and the one-parameter $\mathcal{F}$-$SU(5)$.

In contrast, the squark channels are rather consistent amongst these models. An average branching ratio of about 75% for $\widetilde{q} \to \widetilde{g} + q$ between right-handed squarks $\widetilde{q}_R$ and left-handed squarks $\widetilde{q}_L$ is present throughout the model space, where $\widetilde{q} = (\widetilde{u}, \widetilde{d}, \widetilde{c}, \widetilde{s})$. In one-parameter $\mathcal{F}$-$SU(5)$ and the bino LSP scenario, $\widetilde{t}_1 \to t + \widetilde{\chi}_1^0$ is produced 100% the time, either because $M_{\widetilde{t}_1} < M_{\widetilde{g}}$, or $M_{\widetilde{g}} < M_{\widetilde{t}_1}$ but they nearly degenerate. The situation is not as clean in the remaining model space where the gluino is much lighter than the light stop, as the primary channel for the light stop in each region will be $\widetilde{t}_1 \to \widetilde{g} + t$ at 40% (Higgsino), 36% (Higgs Funnel), and 31% (Mixed).

Table 3.3: Benchmarks of the bino LSP scenario with stau coannihilation and $M_{\tilde{t}_1} < M_{\tilde{g}}$

$M_{1/2}$	1467	1527	1577	1537	1487	1617
M_0	100	160	210	698	648	250
A_0	-1060	-15	-950	-990	-1040	75
M_V	**855**	**915**	**965**	10825	50373	100000
tanβ	18.3	24.3	20.4	34.2	33.7	28.9
m_t	172.9	173.8	174	172.6	172.8	174.1
$M_{\tilde{\chi}_1^0}$	293	308	319	344	353	396
$M_{\tilde{\chi}_2^0/\tilde{\chi}_1^\pm}$	628	658	680	714	725	806
$M_{\tilde{\tau}_1^\pm}$	297	311	322	349	357	397
$M_{\tilde{t}_1}$	1404	1797	1576	1570	1483	1802
$M_{\tilde{u}_R}$	2872	2975	3063	2822	2624	2720
$M_{\tilde{g}}$	1882	1974	2018	2014	2015	2215
M_{H^0}	2850	2580	2940	2220	2060	2130
Ωh^2	0.113	0.111	0.128	0.119	0.115	0.123
Δa_μ	1.48	1.74	1.39	2.14	2.43	2.25
Br$(b \to s\gamma)$	3.49	3.51	3.51	3.4	3.38	3.5
Br$(B_s^0 \to \mu^+\mu^-)$	3.11	3.22	3.18	3.62	3.65	3.34
$\sigma_{\rm SI}$	0.4	0.5	0.3	0.7	1	1.4
$\sigma_{\rm SD}$	1	2	1	3	4	6

Table 3.4: Benchmarks of the bino LSP scenario with stau coannihilation and $M_{\tilde{g}} < M_{\tilde{t}_1}$

$M_{1/2}$	1527	1557	1607	1587
M_0	160	1246	1296	748
A_0	970	3955	4005	3000
M_V	**915**	**945**	**995**	10875
tanβ	28.8	45.1	45.7	39.2
m_t	173.5	173.2	173	174.4
$M_{\tilde{\chi}_1^0}$	308	317	328	357
$M_{\tilde{\chi}_2^0/\tilde{\chi}_1^\pm}$	659	676	700	739
$M_{\tilde{\tau}_1^\pm}$	311	320	331	359
$M_{\tilde{t}_1}$	2009	2500	2572	2197
$M_{\tilde{u}_R}$	2974	3262	3361	2915
$M_{\tilde{g}}$	1984	2052	2114	2095
M_{H^0}	2290	1480	1510	1740
Ωh^2	0.114	0.118	0.117	0.116
Δa_μ	2.02	2.53	2.39	2.59
Br$(b \to s\gamma)$	3.51	3.57	3.57	3.55
Br$(B_s^0 \to \mu^+\mu^-)$	3.27	3.73	3.74	3.52
$\sigma_{\rm SI}$	0.8	5	5	3
$\sigma_{\rm SD}$	4	25	21	17

Table 3.5: Benchmarks of the Higgs Funnel scenario

$M_{1/2}$	2483	2483	2493	2543	1767	1772
M_0	4372	4900	4382	4432	3667	3505
A_0	4900	2930	4910	3975	3889	4116
M_V	**905**	**905**	**915**	10865	53333	93383
tanβ	50	50	51	51.6	51.7	51.6
m_t	172.4	171.8	174.1	173.4	174.1	173.3
$M_{\tilde{\chi}_1^0}$	526	527	529	595	431	441
$M_{\tilde{\chi}_2^0/\tilde{\chi}_1^\pm}$	1021	1049	1109	1206	859	879
$M_{\tilde{\tau}_1^\pm}$	2795	3328	2690	2741	2186	2044
$M_{\tilde{t}_1}$	4733	4880	4702	4428	3243	3162
$M_{\tilde{u}_R}$	6416	6786	6433	6241	4726	4582
$M_{\tilde{g}}$	3332	3349	3340	3348	2484	2515
M_{H^0}	1120	1030	1050	1190	928	945
Ωh^2	0.113	0.0962	0.099	0.112	0.1107	0.1111
Δa_μ	0.81	0.7	0.79	0.76	1.31	1.37
Br$(b \to s\gamma)$	3.75	3.76	3.78	3.71	3.76	3.74
Br$(B_s^0 \to \mu^+\mu^-)$	3.48	3.89	4.09	4.08	3.99	3.88
$\sigma_{\rm SI}$	64	54	27	16	86	77
$\sigma_{\rm SD}$	176	123	52	29	203	177

Table 3.6: Benchmarks of the Higgsino LSP scenario

$M_{1/2}$	2473	2493	2523	2233
M_0	4890	4910	4940	5000
A_0	4890	4910	4940	4556
M_V	**895**	**915**	**945**	80000
tanβ	22.3	46.6	45.1	45.0
m_t	171.7	172.5	171.9	171.0
$M_{\tilde{\chi}_1^0}$	250	260	233	270
$M_{\tilde{\chi}_2^0/\tilde{\chi}_1^\pm}$	256	265	239	276
$M_{\tilde{\tau}_1^\pm}$	4723	3575	3717	3769
$M_{\tilde{t}_1}$	5010	4987	5043	4322
$M_{\tilde{u}_R}$	6790	6813	6864	6225
$M_{\tilde{g}}$	3388	3383	3417	3158
M_{H^0}	5050	2210	2580	2586
Ωh^2	0.0090	0.0096	0.0097	0.0101
Δa_μ	0.24	0.52	0.49	0.55
Br$(b \to s\gamma)$	3.6	3.64	3.62	3.60
Br$(B_s^0 \to \mu^+\mu^-)$	2.98	2.88	2.88	2.84
$\sigma_{\rm SI}$	48	52	47	55
$\sigma_{\rm SD}$	1750	1710	1980	1670

Table 3.7: Benchmarks of the mixed scenario

$M_{1/2}$	2243	1972	2105
M_0	4677	4672	5005
A_0	5010	5005	3894
M_V	40100	66717	86717
tanβ	49.9	50.4	50.4
m_t	171.7	173.3	173.3
$M_{\tilde{\chi}_1^0}$	439	434	477
$M_{\tilde{\chi}_2^0/\tilde{\chi}_1^\pm}$	449	453	496
$M_{\tilde{\tau}_1^\pm}$	3005	2937	3296
$M_{\tilde{t}_1}$	4217	3891	4143
$M_{\tilde{u}_R}$	6006	5718	6100
$M_{\tilde{g}}$	3096	2792	2985
M_{H^0}	892	884	980
Ωh^2	0.0019	0.0008	0.0013
Δa_μ	0.78	0.86	0.75
Br$(b \to s\gamma)$	3.84	3.86	3.81
Br$(B_s^0 \to \mu^+\mu^-)$	2.69	2.74	2.88
$\sigma_{\rm SI}$	81	62	86
$\sigma_{\rm SD}$	382	294	406

3.3 Phenomenological analysis for the D-brane Inspired Soft Terms

The viable parameter space for the D-brane inspired boundary condition is more complicated. The pure scenarios include Higgs Funnel, Higgsino LSP, Stau Coannihilation, and Light Stop Coannihilation. There are also 4 kinds of mixed-of-two scenarios, and 2 mixed-of-three scenarios. FIGs. 3.8-3.11 show how the parameter spaces are filled. We separate the parameter subspace with the relic density falling in one standard deviation from the central value given by WMAP9 and 2015 Planck,

$$0.1134 \leq \Omega h^2 \leq 0.1198 \, . \tag{3.2}$$

FIGs. 3.12-3.15 show the shape of this parameter subspace with respect to different quantities. It is obvious that many empty spaces are taken by points with small relic density.

3.3.1 Classification of viable parameter space

Based on the LSP composition, the viable parameter space can be divided in 9 categories,

1. Stop coannihilation as defined by $M_{\tilde{t}_1} = M_{\text{LSP}}$;
2. Higgsino LSP;
3. Stau coannihilation;
4. Higgs Funnel as defined by $M_{H^0/A^0} = 2M_{\text{LSP}}$;
5. Mixture of Stop coannihilation and Higgsino LSP;
6. Mixture of Higgsino LSP and Stau coannihilation;
7. Mixture of Higgs Funnel and Higgsino LSP;

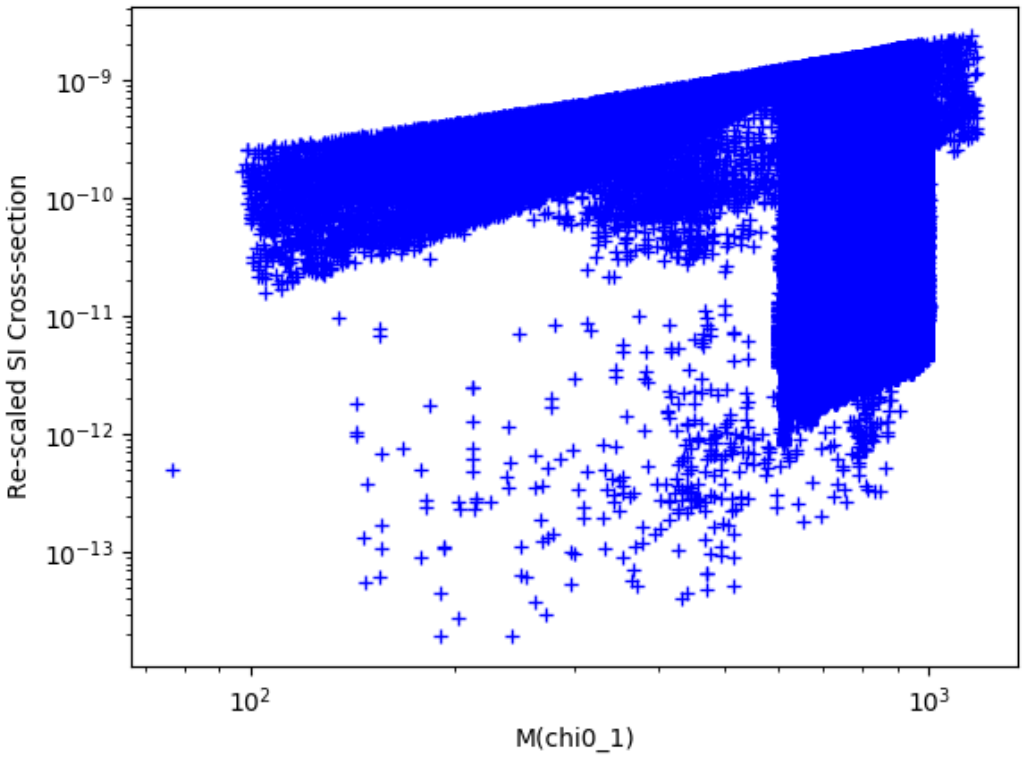

Figure 3.8: Depiction of spin-independent cross-section of the parameter space for the D-brane inspired soft term.

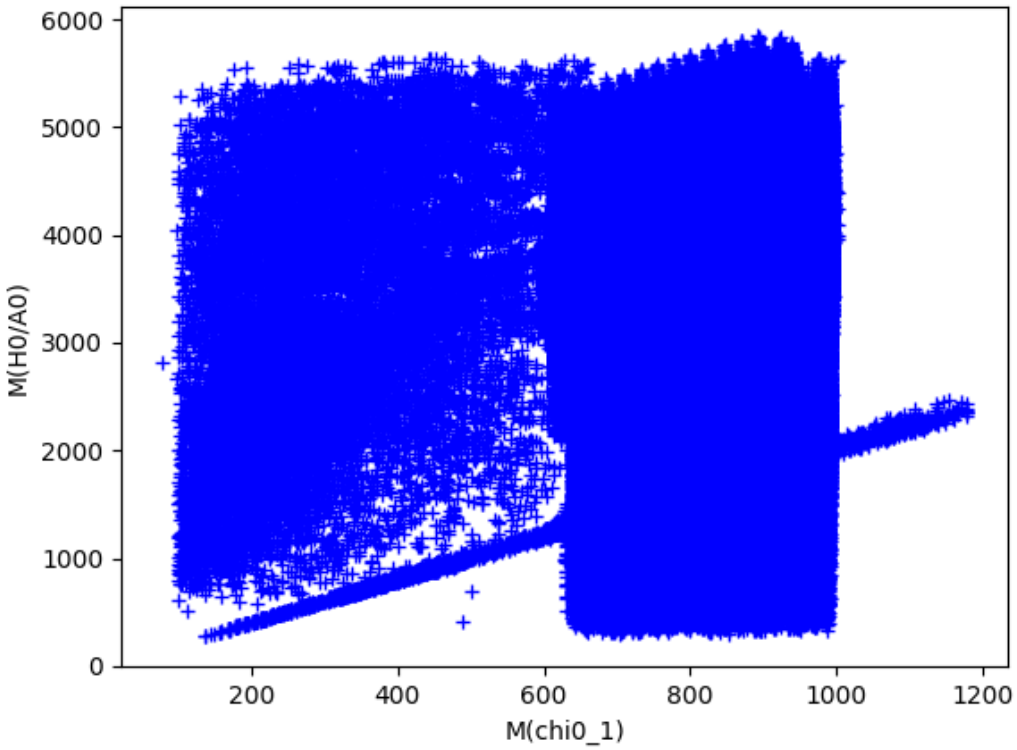

Figure 3.9: Depiction of M_{H^0} as a function of $M_{\chi_1^0}$ of the parameter space for the D-brane inspired soft term.

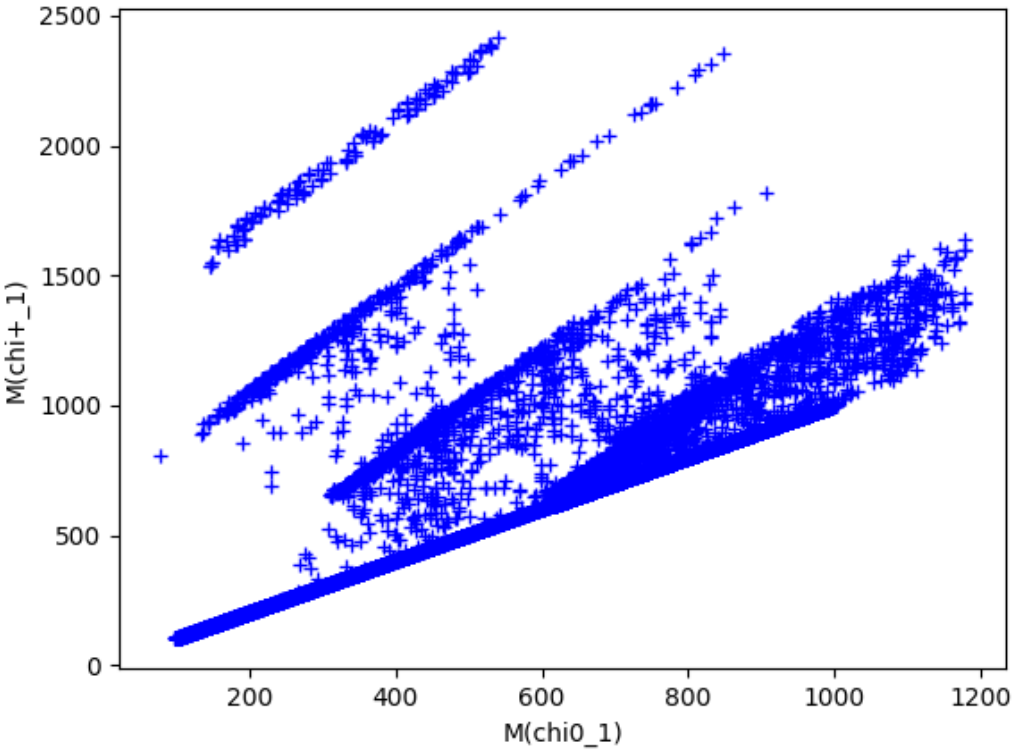

Figure 3.10: Depiction of $M_{\chi_1^\pm}$ as a function of $M_{\chi_1^0}$ of the parameter space for the D-brane inspired soft term.

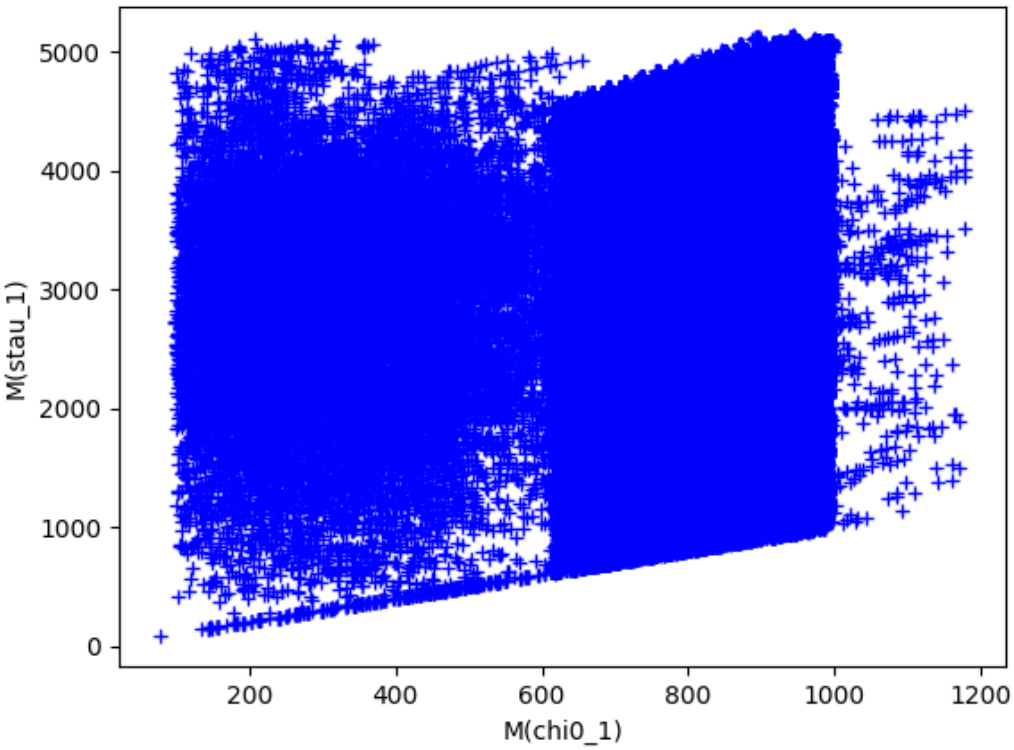

Figure 3.11: Depiction of $M_{\tilde{\tau}_1}$ as a function of $M_{\chi_1^0}$ of the parameter space for the D-brane inspired soft term.

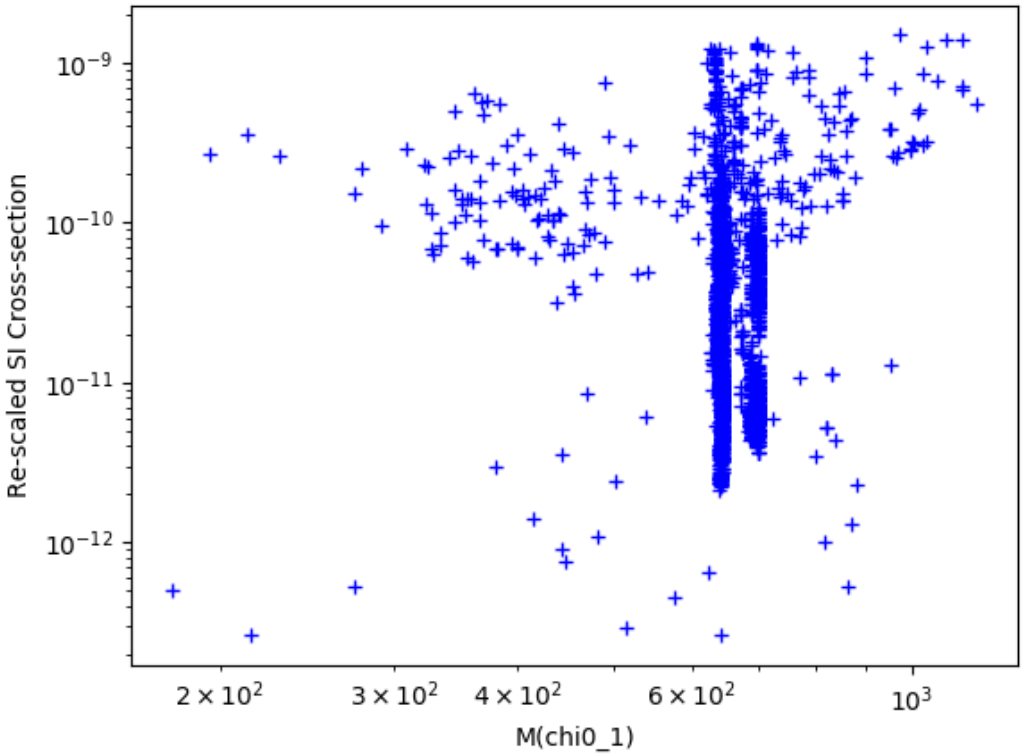

Figure 3.12: Depiction of spin-independent cross-section of the parameter subspace for $0.1134 \leq \Omega h^2 \leq 0.1198$.

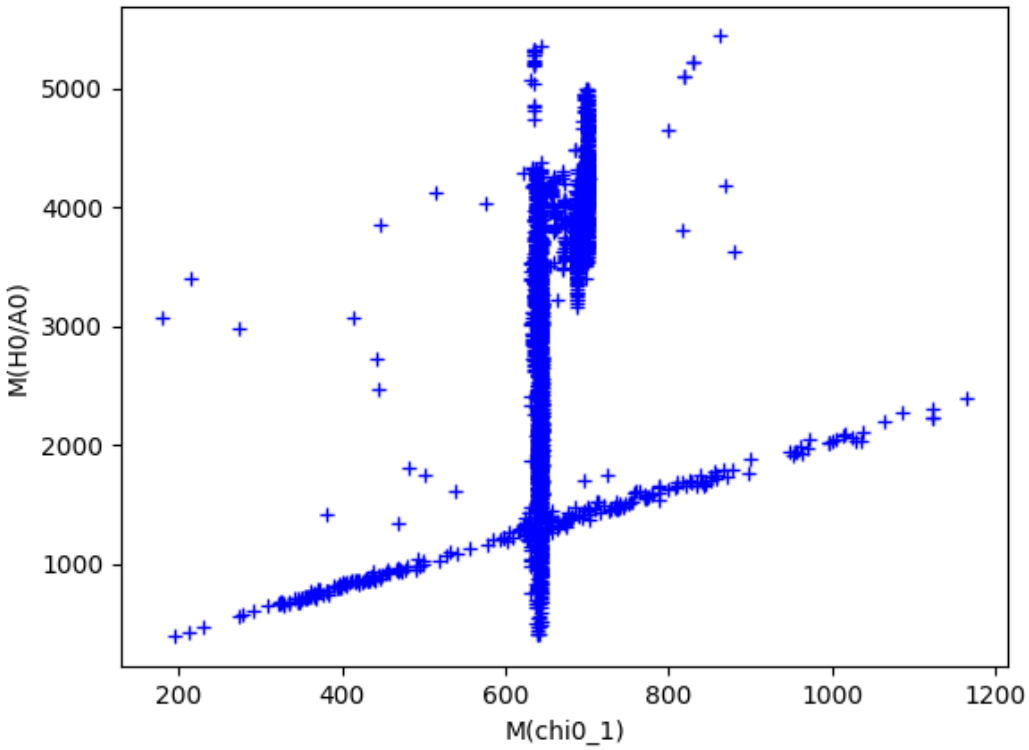

Figure 3.13: Depiction of M_{H^0} as a function of $M_{\chi_1^0}$ of the parameter subspace for $0.1134 \leq \Omega h^2 \leq 0.1198$.

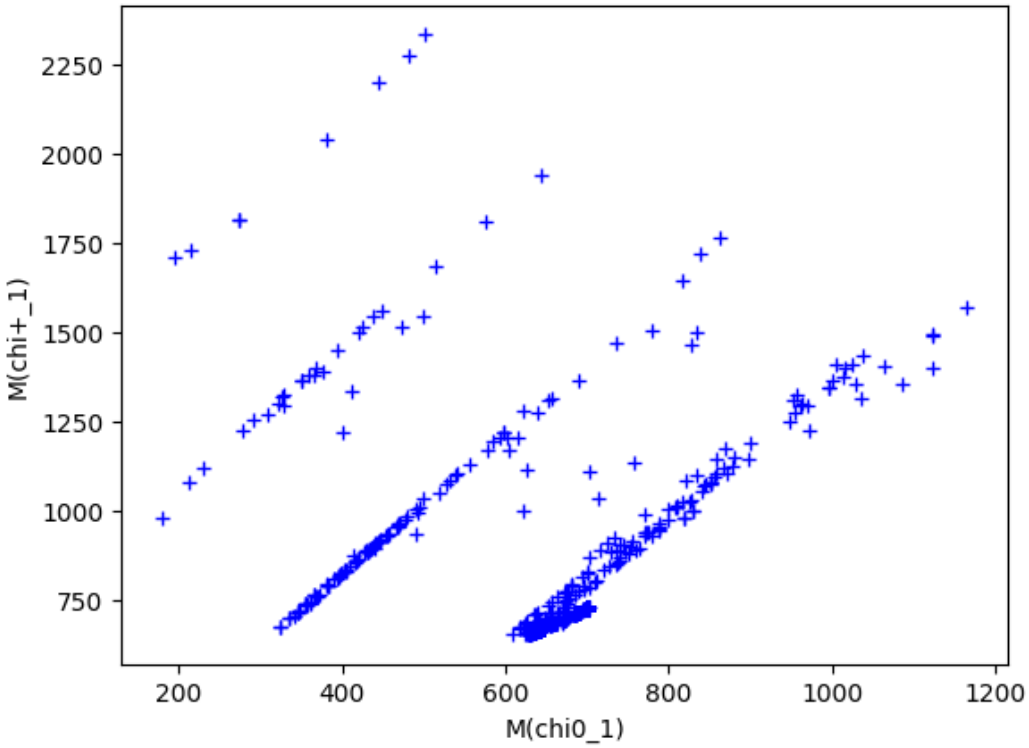

Figure 3.14: Depiction of $M_{\chi_1^\pm}$ as a function of $M_{\chi_1^0}$ of the parameter subspace for $0.1134 \leq \Omega h^2 \leq 0.1198$.

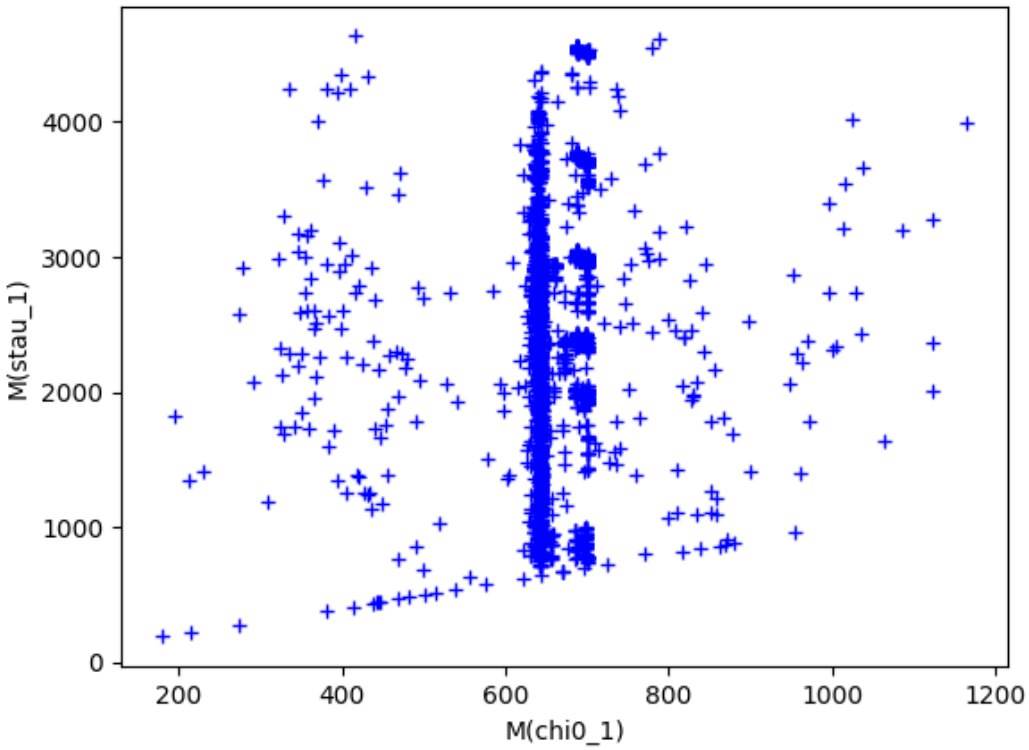

Figure 3.15: Depiction of $M_{\tilde{\tau}_1}$ as a function of $M_{\chi_1^0}$ of the parameter subspace for $0.1134 \leq \Omega h^2 \leq 0.1198$.

8. Mixture of Higgs Funnel and Stau coannihilation;

9. Mixture of Higgs Funnel, Higgsino LSP, and Stau coannihilation.

4. SUMMARY AND CONCLUSIONS

The one-parameter No-Scale $\mathcal{F}$-$SU(5)$ is extended to include General No-Scale Supergravity, allowing the SUSY breaking terms at the unification scale to be generically non-zero. A more diverse phenomenology than the one-parameter $\mathcal{F}$-$SU(5)$ is revealed by the numerical scan of the parameter space. The DM searching results directly distinguish different physics in our parameter space of general No-Scale boundary conditions in the $\mathcal{F}$-$SU(5)$ model with mSUGRA/CMSSM soft terms. A special parameter region that exhibits both Higgs Funnel and Higgsino LSP scenarios is found. The benchmark points show interesting spectra and decay modes to be tested by the next run of LHC.

REFERENCES

[1] Wikipedia, "Standard model of elementary particles," April 2017. en.wikipedia.org/wiki/Standard_Model.

[2] Wikipedia, "Hierarchy problem," January 2008. en.wikipedia.org/wiki/Hierarchy_problem.

[3] R. P. Feynman, R. B. Leighton, and M. Sands, *The Feynman Lectures on Physics*, vol. I, ch. 1, p. 2. Addison-Wesley, 1964.

[4] K. Huang, *QUARKS, LEPTONS AND GAUGE FIELDS*. 1982.

[5] T. D. Lee and C.-N. Yang, "Question of Parity Conservation in Weak Interactions," *Phys. Rev.*, vol. 104, pp. 254–258, 1956.

[6] C. S. Wu, E. Ambler, R. W. Hayward, D. D. Hoppes, and R. P. Hudson, "Experimental Test of Parity Conservation in Beta Decay," *Phys. Rev.*, vol. 105, pp. 1413–1414, 1957.

[7] S. P. Martin, "A Supersymmetry primer," 1997. [Adv. Ser. Direct. High Energy Phys.18,1(1998)].

[8] J. Wess and J. Bagger, *Supersymmetry and supergravity*. 1992.

[9] R. N. Mohapatra, *Unification and Supersymmetry*. Springer, 2002.

[10] H. Georgi and S. L. Glashow, "Unity of All Elementary-Particle Forces," *Phys. Rev. Lett.*, vol. 32, p. 438, 1974.

[11] H. Nishino *et al.*, "Search for Proton Decay via $p \to e + \pi^0$ and $p \to \mu^+\pi^0$ in a Large Water Cherenkov Detector," *Phys. Rev. Lett.*, vol. 102, p. 141801, 2009.

[12] S. M. Barr, "A New Symmetry Breaking Pattern for $SO(10)$ and Proton Decay," *Phys. Lett.*, vol. B112, p. 219, 1982.

[13] J. P. Derendinger, J. E. Kim, and D. V. Nanopoulos, "Anti-$SU(5)$," *Phys. Lett.*, vol. B139, p. 170, 1984.

[14] I. Antoniadis, J. R. Ellis, J. S. Hagelin, and D. V. Nanopoulos, "Supersymmetric Flipped $SU(5)$ Revitalized," *Phys. Lett.*, vol. B194, p. 231, 1987.

[15] J. Jiang, T. Li, and D. V. Nanopoulos, "Testable Flipped $SU(5) \times U(1)_X$ Models," *Nucl. Phys.*, vol. B772, pp. 49–66, 2007.

[16] J. Jiang, T. Li, D. V. Nanopoulos, and D. Xie, "F-$SU(5)$," *Phys. Lett.*, vol. B677, pp. 322–325, 2009.

[17] J. Jiang, T. Li, D. V. Nanopoulos, and D. Xie, "Flipped $SU(5) \times U(1)_X$ Models from F-Theory," *Nucl. Phys.*, vol. B830, pp. 195–220, 2010.

[18] E. Cremmer, S. Ferrara, C. Kounnas, and D. V. Nanopoulos, "Naturally Vanishing Cosmological Constant in $N = 1$ Supergravity," *Phys. Lett.*, vol. B133, p. 61, 1983.

[19] J. R. Ellis, A. B. Lahanas, D. V. Nanopoulos, and K. Tamvakis, "No-Scale Supersymmetric Standard Model," *Phys. Lett.*, vol. B134, p. 429, 1984.

[20] J. R. Ellis, C. Kounnas, and D. V. Nanopoulos, "Phenomenological $SU(1,1)$ Supergravity," *Nucl. Phys.*, vol. B241, p. 406, 1984.

[21] J. R. Ellis, C. Kounnas, and D. V. Nanopoulos, "No Scale Supersymmetric Guts," *Nucl. Phys.*, vol. B247, pp. 373–395, 1984.

[22] A. B. Lahanas and D. V. Nanopoulos, "The Road to No Scale Supergravity," *Phys. Rept.*, vol. 145, p. 1, 1987.

[23] ATLAS, "Exotics combined summary plots," 2016. atlas.web.cern.ch/Atlas/ /GROUPS/PHYSICS/CombinedSummaryPlots/EXOTICS/index.html.

[24] T. A. Aaltonen, "Combination of CDF and DO results on the mass of the top quark using up to 8.7 fb^{-1} at the Tevatron," 2013.

[25] G. Belanger, F. Boudjema, A. Pukhov, and A. Semenov, "Dark matter direct detection rate in a generic model with micrOMEGAs2.1," *Comput. Phys. Commun.*, vol. 180, pp. 747–767, 2009.

[26] A. Djouadi, J.-L. Kneur, and G. Moultaka, "SuSpect: A Fortran code for the supersymmetric and Higgs particle spectrum in the MSSM," *Comput. Phys. Commun.*, vol. 176, pp. 426–455, 2007.

[27] G. Aad *et al.*, "Observation of a new particle in the search for the Standard Model Higgs boson with the ATLAS detector at the LHC," *Phys.Lett.*, vol. B716, pp. 1–29, 2012.

[28] S. Chatrchyan *et al.*, "Observation of a new boson at a mass of 125 GeV with the CMS experiment at the LHC," *Phys.Lett.*, vol. B716, pp. 30–61, 2012.

[29] G. Hinshaw *et al.*, "Nine-Year Wilkinson Microwave Anisotropy Probe (WMAP) Observations: Cosmological Parameter Results," 2012.

[30] P. Ade *et al.*, "Planck 2015 results. XIII. Cosmological parameters," 2015.

[31] W. Adam, "Searches for SUSY, talk at the 38th International Conference on High Energy Physics," 2016.

[32] HFAG, 2013. www.slac.stanford.edu/xorg/hfag/rare/2013/radll/OUTPUT/ TABLES/ /radll.pdf.

[33] V. Khachatryan *et al.*, "Search for Supersymmetry in pp Collisions at 7 TeV in Events with Jets and Missing Transverse Energy," *Phys.Lett.*, vol. B698, pp. 196–218, 2011.

[34] T. Aoyama, M. Hayakawa, T. Kinoshita, and M. Nio, "Complete Tenth-Order QED Contribution to the Muon g-2," *Phys.Rev.Lett.*, vol. 109, p. 111808, 2012.

[35] E. Behnke *et al.*, "First Dark Matter Search Results from a 4-kg CF_3I Bubble Chamber Operated in a Deep Underground Site," *Phys. Rev.*, vol. D86, no. 5, p. 052001, 2012. [Erratum: Phys. Rev.D90,no.7,079902(2014)].

[36] E. Aprile *et al.*, "Limits on spin-dependent WIMP-nucleon cross sections from 225 live days of XENON100 data," *Phys. Rev. Lett.*, vol. 111, no. 2, p. 021301, 2013.

[37] D. S. Akerib *et al.*, "Results from a search for dark matter in LUX with 332 live days of exposure," 2016.

[38] A. Tan *et al.*, "Dark Matter Results from First 98.7-day Data of PandaX-II Experiment," *Phys. Rev. Lett.*, vol. 117, no. 12, p. 121303, 2016.

[39] M.M. Mühlleitner, A. Djouadi, and M. Spira, "Decays of Supersymmetric Particles: the program SUSY-HIT (SUspect-SdecaY-Hdecay-InTerface)," *Acta Phys. Polon.*, vol. B38, pp. 635–644, 2007.

APPENDIX A

GENERATORS OF $SU(3)$

The generators of $SU(3)$ are $T_a = \lambda_a$, where the λ's are given by the Gell-Mann matrices.

A.1 Gell-Mann Matrices

The Gell-Mann matrices are analog to Pauli matrices of $SU(2)$ group. They are given by,

$$\lambda_1 = \begin{pmatrix} 0 & 1 & 0 \\ 1 & 0 & 0 \\ 0 & 0 & 0 \end{pmatrix} , \tag{A.1}$$

$$\lambda_2 = \begin{pmatrix} 0 & -i & 0 \\ i & 0 & 0 \\ 0 & 0 & 0 \end{pmatrix} , \tag{A.2}$$

$$\lambda_3 = \begin{pmatrix} 1 & 0 & 0 \\ 0 & -1 & 0 \\ 0 & 0 & 0 \end{pmatrix} , \tag{A.3}$$

$$\lambda_4 = \begin{pmatrix} 0 & 0 & 1 \\ 0 & 0 & 0 \\ 1 & 0 & 0 \end{pmatrix} , \tag{A.4}$$

$$\lambda_5 = \begin{pmatrix} 0 & 0 & -i \\ 0 & 0 & 0 \\ i & 0 & 0 \end{pmatrix} , \tag{A.5}$$

$$\lambda_6 = \begin{pmatrix} 0 & 0 & 0 \\ 0 & 0 & 1 \\ 0 & 1 & 0 \end{pmatrix} , \tag{A.6}$$

$$\lambda_7 = \begin{pmatrix} 0 & 0 & 0 \\ 0 & 0 & -i \\ 0 & i & 0 \end{pmatrix} , \tag{A.7}$$

$$\lambda_8 = \frac{1}{\sqrt{3}} \begin{pmatrix} 1 & 0 & 0 \\ 0 & 1 & 0 \\ 0 & 0 & -2 \end{pmatrix} . \tag{A.8}$$

A.2 Commutators and Anticommutators of the Generators of $SU(3)$

The commutators the generators of $SU(3)$ are

$$[T_a, T_b] = i \sum_{c=1}^{8} f_{abc} T_c , \tag{A.9}$$

where the f's are the structure constants of the $\mathfrak{su}(3)$ Lie algebra, and are given by

$$f_{123} = 1 , \tag{A.10}$$

$$f_{147} = -f_{156} = f_{246} = f_{257} = f_{345} = -f_{367} = \frac{1}{2} , \tag{A.11}$$

$$f_{458} = f_{678} = \frac{\sqrt{3}}{2} \, . \tag{A.12}$$

The anticommutators the generators of $SU(3)$ are

$$\{T_a, T_b\} = \frac{1}{3}\delta_{ab} + \sum_{c=1}^{8} d_{abc} T_c \, , \tag{A.13}$$

where the d's are given by

$$d_{118} = d_{228} = d_{338} = -d_{888} = \frac{1}{\sqrt{3}} \, , \tag{A.14}$$

$$d_{448} = d_{558} = d_{668} = d_{778} = -\frac{1}{2\sqrt{3}} \, , \tag{A.15}$$

$$d_{146} = d_{157} = -d_{247} = d_{256} = d_{344} = d_{355} = -d_{366} = -d_{377} = \frac{1}{2} \, . \tag{A.16}$$

APPENDIX B

MATRIX FORM OF BOSON REPRESENTATIONS OF GEORGI-GLASHOW $SU(5)$

The first 8 matrices are the same as the Gell-Mann matrices of $SU(3)$ group in Appendix A, except that the two added dimensions are all zeros,

$$\lambda_i = \begin{pmatrix} \lambda_i & O_{3\times 2} \\ O_{2\times 3} & O_{2\times 2} \end{pmatrix} \ , \ i = 1, 2, \cdots, 8. \tag{B.1}$$

The next 12 matrices are in the form of

$$\lambda_i = \begin{pmatrix} O_{3\times 3} & A_i \\ A_i^T & O_{2\times 2} \end{pmatrix} \ , \ i = 9, 10, \cdots, 20, \tag{B.2}$$

where A_i's are

$$A_9 = \begin{pmatrix} 1 & 0 \\ 0 & 0 \\ 0 & 0 \end{pmatrix} \ , \ A_{10} = \begin{pmatrix} -i & 0 \\ 0 & 0 \\ 0 & 0 \end{pmatrix} \ , \tag{B.3}$$

$$A_{11} = \begin{pmatrix} 0 & 1 \\ 0 & 0 \\ 0 & 0 \end{pmatrix} \ , \ A_{12} = \begin{pmatrix} 0 & -i \\ 0 & 0 \\ 0 & 0 \end{pmatrix} \ , \tag{B.4}$$

$$A_{13} = \begin{pmatrix} 0 & 0 \\ 1 & 0 \\ 0 & 0 \end{pmatrix} \ , \ A_{14} = \begin{pmatrix} 0 & 0 \\ -i & 0 \\ 0 & 0 \end{pmatrix} \ , \tag{B.5}$$

$$A_{15} = \begin{pmatrix} 0 & 0 \\ 0 & 1 \\ 0 & 0 \end{pmatrix} \ , \ A_{16} = \begin{pmatrix} 0 & 0 \\ 0 & -i \\ 0 & 0 \end{pmatrix} \ , \tag{B.6}$$

$$A_{17} = \begin{pmatrix} 0 & 0 \\ 0 & 0 \\ 1 & 0 \end{pmatrix} \ , \ A_{18} = \begin{pmatrix} 0 & 0 \\ 0 & 0 \\ -i & 0 \end{pmatrix} \ , \tag{B.7}$$

$$A_{19} = \begin{pmatrix} 0 & 0 \\ 0 & 0 \\ 0 & 1 \end{pmatrix} \ , \ A_{20} = \begin{pmatrix} 0 & 0 \\ 0 & 0 \\ 0 & -i \end{pmatrix} \ . \tag{B.8}$$

The next 3 matrices are made by putting Pauli matrices in the fourth and fifth dimension,

$$\lambda_{20+i} = \begin{pmatrix} O_{3\times 3} & O_{3\times 2} \\ O_{2\times 3} & \tau_i \end{pmatrix} \ , \ i = 1, 2, 3. \tag{B.9}$$

The last one is

$$\lambda_{24} = \frac{2}{\sqrt{15}} \text{diag} \left(1, 1, 1, -\frac{3}{2}, -\frac{3}{2} \right) \ . \tag{B.10}$$